NASA/TM—2008–215579

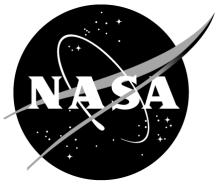

Micro- and Nanostructured Metal Oxide Chemical Sensors for Volatile Organic Compounds

M.A. Alim, B.G. Penn, and J.R. Currie, Jr.
Marshall Space Flight Center, Marshall Space Flight Center, Alabama

A.K. Batra and M.D. Aggarwal
Alabama A&M University, Normal, Alabama

October 2008

The NASA STI Program…in Profile

Since its founding, NASA has been dedicated to the advancement of aeronautics and space science. The NASA Scientific and Technical Information (STI) Program Office plays a key part in helping NASA maintain this important role.

The NASA STI program operates under the auspices of the Agency Chief Information Officer. It collects, organizes, provides for archiving, and disseminates NASA's STI. The NASA STI program provides access to the NASA Aeronautics and Space Database and its public interface, the NASA Technical Report Server, thus providing one of the largest collections of aeronautical and space science STI in the world. Results are published in both non-NASA channels and by NASA in the NASA STI Report Series, which includes the following report types:

- TECHNICAL PUBLICATION. Reports of completed research or a major significant phase of research that present the results of NASA programs and include extensive data or theoretical analysis. Includes compilations of significant scientific and technical data and information deemed to be of continuing reference value. NASA's counterpart of peer-reviewed formal professional papers but has less stringent limitations on manuscript length and extent of graphic presentations.

- TECHNICAL MEMORANDUM. Scientific and technical findings that are preliminary or of specialized interest, e.g., quick release reports, working papers, and bibliographies that contain minimal annotation. Does not contain extensive analysis.

- CONTRACTOR REPORT. Scientific and technical findings by NASA-sponsored contractors and grantees.

- CONFERENCE PUBLICATION. Collected papers from scientific and technical conferences, symposia, seminars, or other meetings sponsored or cosponsored by NASA.

- SPECIAL PUBLICATION. Scientific, technical, or historical information from NASA programs, projects, and missions, often concerned with subjects having substantial public interest.

- TECHNICAL TRANSLATION. English-language translations of foreign scientific and technical material pertinent to NASA's mission.

Specialized services also include creating custom thesauri, building customized databases, and organizing and publishing research results.

For more information about the NASA STI program, see the following:

- Access the NASA STI program home page at <http://www.sti.nasa.gov>

- E-mail your question via the Internet to <help@sti.nasa.gov>

- Fax your question to the NASA STI Help Desk at 443–757–5803

- Phone the NASA STI Help Desk at 443–757–5802

- Write to:
  NASA STI Help Desk
  NASA Center for AeroSpace Information
  7115 Standard Drive
  Hanover, MD 21076–1320

NASA/TM—2008–215579

Micro- and Nanostructured Metal Oxide Chemical Sensors for Volatile Organic Compounds

M.A. Alim, B.G. Penn, and J.R. Currie, Jr.
Marshall Space Flight Center, Marshall Space Flight Center, Alabama

A.K. Batra and M.D. Aggarwal
Alabama A&M University, Normal, Alabama

National Aeronautics and
Space Administration

Marshall Space Flight Center • MSFC, Alabama 35812

October 2008

TRADEMARKS

Available from:

NASA Center for AeroSpace Information
7115 Standard Drive
Hanover, MD 21076–1320
443–757–5802

This report is also available in electronic form at
<https://www2.sti.nasa.gov>

TABLE OF CONTENTS

TABLE OF CONTENTS (Continued)

LIST OF FIGURES

LIST OF FIGURES (Continued)

LIST OF FIGURES (Continued)

LIST OF ACRONYMS AND SYMBOLS

θ	depression angle
AAMU	Alabama A&M University
AC/DC	alternating current / direct current
APM	acoustic plane mode
Au	gold
°C	degrees Celsius
CH_3-CHOH-CH_3 or IPA	isopropyl alcohol (or isopropanol)
CH_4	methane
ChemFET	chemical field effect transistor
CMOS	metal oxide semiconductor
CO	carbon monoxide
CO_X	oxides of carbon
DMMP	dimethyl methyl phosphonate
e–	charged electron
E_C	conduction band
E_F	Fermi level
E_V	valance band
f	frequency
FET	field effect transistor
FPW	flexural plane wave

LIST OF ACRONYMS AND SYMBOLS (Continued)

Ga_2O_3	gallium oxide
H_2	molecular hydrogen
H_2S	hydrogen sulfide
In_2O_3	indium oxide
IPA or CH_3-CHOH-CH_3	isopropyl alcohol (or isopropanol)
LPG	liquefied petroleum gas
MHz	mega hertz
MO	metal oxide
MOS	metal oxide semiconductor
N_2	nitrogen gas
NH_3	ammonia
NOX	oxides of nitrogen
O_2	gaseous oxygen
O_{ads}^-	adsorbed oxygen
O_L	lattice oxygen
Pd	palladium
ppb	part per billion
ppm	part per million
Pt	platinum
R (g)	reducing gas
RO (g)	oxidized reducing gas

LIST OF ACRONYMS AND SYMBOLS (Continued)

R_G	sensor resistance under the influence of a target gas
R_A	sensor resistance in the reference atmosphere
RTV	silicone adhesive
Ru	ruthenium
S	sensitivity
SAW	surface acoustic wave
SMO	semiconductor metal oxide
SnO_2	tin oxide
SO_X	oxides of sulfur
SPR	surface plasmon resonance
TiO_2	titanium oxide
TFT	thick-film transfer
TIO	tin oxide - indium oxide
TSM	thickness sheer mode
TTO	tin oxide - tungsten oxide
TWC	three-way catalyst
TZO	tin oxide - zinc oxide
WO_3	tungsten oxide
YSZ	yttria stabilized zirconia
ZnO	zinc oxide
ZrO_2	zirconia (zirconium dioxide or zirconium oxide)

NOMENCLATURE

α	finite value of exponent depression parameter
F	farad
cm	centimeter
°C	degree Celsius
°C/min	degree Celsius per minute
D	diameter of depleted crystallite
j	square root of {–1} or sqrt of {–1}
L	depth of depleted electron layer
liter	volume unit of fluid
λ_D	Debye length
M	metal cation
MΩ	megohm (10^6 ohm)
μm	micro-meter (or 10^{-6} meter)
nm	nanometer (or 10^{-9} meter)
τ	relaxation time
Z'	real part of Z
Z''	imaginary part of Z
Z_∞	resistance at the high frequency limit
ω	angular frequency

TECHNICAL MEMORANDUM

MICRO- AND NANOSTRUCTURED METAL OXIDE CHEMICAL SENSORS FOR VOLATILE ORGANIC COMPOUNDS

1. INTRODUCTION

Emulation of human senses has always been a technological goal. There are cameras to mimic the eyes, microphones that mimic the ears, tactile sensors to mimic touch, and chemical sensors to mimic the nose and tongue. In today's world, there is growing interest in developing chemical sensors for industrial use. Applications include monitoring air pollution and hazardous gas detection under several situations in mines and other confined spaces, gradation of agricultural products, such as coffee and spices, alcoholic beverage production, hand-held breath analyzers, exhaust gas monitoring, etc.

Sensors are devices that are composed of an active sensing material with a signal transducer. The role of these two important components in sensors is to transmit signal without any amplification from a selective compound or from a change in a reaction. These devices produce any one of the electrical or thermal or optical output signals which could be converted to the digital signals for subsequent processing. Classifying sensing devices achieved are based on these output signals. Among these sensors, electrochemical sensors have more advantages over other types of sensing devices. This is because the electrodes can sense materials which are present within the host without any damage or degradation to the host system.

Gas sensors based on wide band-gap semiconductor metal oxides are playing an important role in the detection of toxic pollutants (H_2S, CO_X, NO_X, SO_X, etc.) and combustible gases (H_2, CH_4, other hydrocarbons, alcohols, and flammable organic vapors). Metal oxides such as tin oxide (SnO_2), zinc oxide (ZnO), titanium dioxide (TiO_2), tungsten oxide (WO_3), gallium oxide (Ga_2O_3), and other cationic oxides have been examined for gas-sensing purposes in order to provide feedback for the control of industrial processes. Among these, SnO_2 is a widely studied material.[1–7] It is well-known that the adsorption of gas on the surface of a semiconductor can cause changes in resistance, as well as in capacitance. The detection principle of the resistive sensors is based on changes of the resistance of a metal oxide thin-film semiconductor upon adsorption of the gas molecules. The adsorbed gas molecules can then be easily detected from the change in magnitude.

The gas-solid interaction influences the density of electronic species in the film and thereby affects the resistance of the film. Metal-oxide-based sensing materials are also sometimes called chemiresistors. These are the simplest form of the gas sensors among various technologies and are perhaps the most attractive type of portable applications. They have the advantage of achieving

compact size via fabrication method at low cost and simple measurement electronics. However, ease of fabrication of a chemiresistor is offset by inherent limitations in selectivity and sensitivity. Chemiresistors tend to be broadly selective and respond to a large variety of gases. Fortunately, the response to these gases can be tuned by modifying a range of parameters, such as adding catalysts, doping, and manipulating microstructure with grain-size through sintering cycles, including external filters controlling operating temperature.[8]

There is a strong need for sensors having an ultra-low response time and sharp sensitivity to avoid catastrophic accidents in the space industry due to leakage in the propellant systems of the aircrafts, rockets, engines, etc. Furthermore, there is a need to simplify the manufacturing processes of these sensing materials to achieve miniaturized sensors, while improving the sensing characteristics of the metal oxides, including lowering the operating temperature. Recently, it has been reported that the composite sensors incorporating different proportions of SnO_2 and ZnO exhibit higher sensitivity for a large range of organic vapors.[9] Most importantly, the composite sensors have shown to possess significantly higher sensitivity than the sensors prepared from single constituent SnO_2 or ZnO, operated under identical experimental conditions. The increase in sensitivity is caused from the synergistic effects documented as the complementary catalytic activity[10] in conjunction with the formation of hetero-junctions that combined with the changes in microstructure during sintering.[11]

Alabama A&M University (AAMU) recently undertook systematic investigation regarding the fabrication of thick-film sensing materials comprised of binary oxide constituents, such as SnO_2-ZnO, SnO_2-In_2O_3, SnO_2-WO_3, etc. Scientists conducted experiments to examine the sensitivity and response time of 2-isopropanol.[12] Basically; this research on organic volatile compound vapor sensor was aimed at obtaining new material systems to achieve highly sensitive devices with lower operating temperature and to predict the detection capability of sensing materials for different concentrations. This technical memorandum (TM) presents the results.

This TM is focused on various gas-sensing technologies, mechanisms, principles of operating semiconducting metal-oxide-gas-sensing materials, sensing parameters, and factors influencing their performance. This TM also notes the description of the apparatus designed, constructed, and used for testing organic volatile compounds at AAMU.[12] This TM also presents the processing methods and/or pertinent fabrication steps, including the results of the performance of the binary metal oxides under the influence of 2-isopropanol, satisfying reasonable mechanisms of detection. Based on the results of the binary systems, this TM reviews the main research direction of nanoscience and nanotechnology applied to the semiconductor gas sensors are reviewed attributing to SnO_2. Thus, researchers characterized SnO_2 as a single-phase material.[13]

2. REVIEW OF GAS-SENSING TECHNOLOGIES

Experimenters have performed many research and development activities regarding small, low mass, compact geometry, and inexpensive gas sensors. These activities include processing; characterization; evaluation of sensitivity, effectiveness, response time, and stability with respect to specific application; likelihood of degradation; etc. Basing their work upon various principles and operation mechanisms, researchers have developed a large number of semiconducting sensors, such as gas sensors; optical sensors; thermal-conductivity sensors; and mass-sensitivity devices, like quartz microbalance sensors, catalytic sensors, dielectric sensors, electrochemical sensors, and electrolyte sensors. Typically, the gas of interest interacts or adsorbs onto the surface of a sensitive material, thereby inducing a change in the electrical behavior of the material that in turn is the measure of gas concentration. The electrical parameters can be extracted from a wide variety of measurements, including AC/DC resistance, overall impedance affecting terminal capacitance, field effect transistor (FET) threshold voltages, phase change of a wave propagated across the sensor surface (surface acoustic wave sensors), resonant frequency of cantilever beams, and so on. This TM describes the methodological perspective of a few technologies.

2.1 Metal-Oxide-Based Gas-Sensing Materials

The detection principle of the resistive sensors is based on changes of the resistance of a metal oxide thin-film, which is usually semiconducting in nature. The change of the resistance takes place upon adsorption of the gas molecules onto the surface of the sensing material. The gas-solid interactions influence the density of electronic species in the film and thereby the resistance of the film. The metal-oxide-based sensor is also sometimes referred to as a chemiresistor. It is the simplest type of gas sensor among various technologies and, hence, is perhaps the most attractive for portable applications. The sensing material possesses the advantages of compact size, simple fabrication method, low cost, and holding simple measurement electronics.

Simplicity of fabrication of the chemiresistor, however, is offset by inherent limitations in selectivity and sensitivity. The chemiresistors tend to be broadly selective, responding to a large family of gases. The sensing properties are related to the surface reaction between the species to be detected and adsorbed oxygen. The physical quantity normally measured is the resistance, which depends on the adsorbed species through the height of energy barriers between the grains. The applications of semi-conducting gas sensors range from environmental monitoring and automotive application to domestic and industrial applications. The benefits offered by the semiconductor gas sensors are related mainly to small geometry, cost, and the possibility of online operation. A typical design of a metal oxide sensor is illustrated in figure 1:

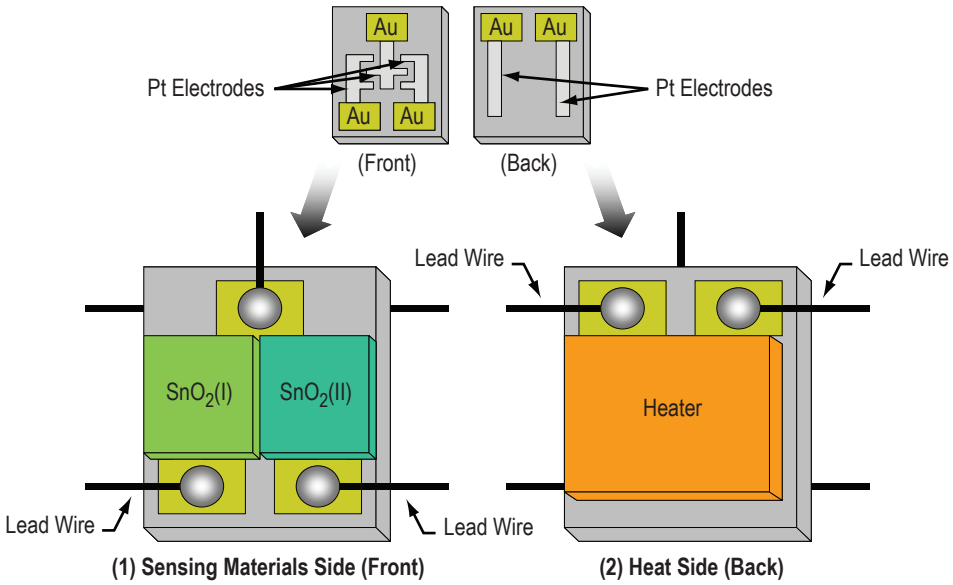

Figure 1. The design of a typical metal oxide chemical sensor.

2.2 Capacitance-Based Sensors

Capacitive-type gas sensors measure the change in dielectric constant of films between the electrodes as a function of gas concentration. The change of capacitance in the sensor is typically on the order of 10^{-12} F, dependent on the operating frequency and surrounding conditions, such as temperature and humidity. This type of sensor relies on inter-digitated electrode structures that correspond to the two plates of a standard capacitor to monitor changes of the dielectric coefficient of the film.[14] If the capacitance of the film is lower than that of the analyte, then the capacitance will increase, and if the capacitance of the film is higher than the analyte, then the capacitance will decrease.

2.3 Acoustic-Wave-Based Sensors

Acoustic wave sensors are very versatile. Due to the high sensitivity of the sensor to surface mass changes, they have many applications as gas sensors, biological sensors, and tactile sensors.[15,16] Types of acoustic sensors[17] include thickness shear mode (TSM), surface acoustic wave (SAW), flexural plane wave (FPW),[18,19] and acoustic plane mode (APM). All these sensors use piezoelectric materials in the form of thin-films or bulk to launch the acoustic waves. Plenty of literature is available with these devices used as gas sensors.[20–24] Recently, Analytical Chemistry published a pair of comprehensive articles that deal with various acoustic sensors.[25,26] A typical acoustic device consists of a piezoelectric material[27–29] with one or more transducers on its surface(s). These transducers launch acoustic waves into the material at frequencies that may range from few MHz to hundreds of MHz. The crystal or film orientation, thickness of piezoelectric material, and the geometry of the metal transducers[30,31] determine the type of acoustic wave generated and the device's resonant frequency. Depending on the device and the type of wave generated, it is possible to obtain properties and measure processes of the chemical species in the gas

phase, liquid phase in vacuum, thin solid films, etc. Various researchers have provided an analytical comparison among the various acoustic sensors.[32,33]

A chemical reacts with a chemically selective layer on the sensor surface causing a frequency, phase, or amplitude shift in the acoustic wave traveling across the device.[34] Piezoelectric behavior, acoustic coupling, or similar means can generate the wave itself.[17] The SAW sensors[17,35,36] often experience prohibitively long response times for many chemical-sensing applications.[37] Also, acoustic wave devices require high frequencies of operation at smaller sizes, complicating the readout electronics and incurring stringent constraints on impedance matching and noise management. Instead of one sensitive layer, developers can use a dual-layer structure in sensing material, as has been reported for hydrogen detection,[38] which makes possible the detection of gas species even at room temperature. There is a reported use of two different sensitive materials, copper phthalocyanine and palladium, in a single SAW sensor. Another important acoustic-wave-based sensor is the flexural plane wave sensor, in which the device plane thickness is only a few percent of the acoustic wavelength. This offers an improved behavior over SAW devices in terms of sensitivity and response time, allowing complete isolation of the electronics from the medium being investigated and, more importantly, feasibility of operating in liquid medium.[17,20,39] These devices are analogous to the SAW sensor, but can be fabricated on silicon and integrated along with microelectronics.

2.4 FET-Based Sensor

The development of semiconductor technology has led to the emergence of semiconductor chemical sensors. Semiconductor chemical sensors are based on the metal oxide semiconductor (MOS) junction principle. These MOSFET-based gas sensors are complex solid-state gas sensors and are inherently more complex to fabricate and require more extensive control and measurement electronics. FETs can be fabricated in standard CMOS and other micro-fabrication processes, and conversion of the electronic FET to an effective sensor requires, in theory, only replacement of the gate with a suitable chemically sensitive material. Environment, material compatibility, and other fabrication issues, however, make the integration of the chemical FET (ChemFET) architectures significantly more complicated than the theory. Because of the convenience and compatibility of the FET structure with standard microfabrication processes, the ChemFET continues to be pursued as a viable solution to chemical-sensing problems requiring portability and real time operation. The ChemFET uses a standard oxide layer and a chemically sensitive metal, such as palladium as gate.[40]

2.5 Calorimetric-Based Sensors

Calorimetric gas sensors burn combustible gases with the surrounding air on the surface of a film of a catalytically active metal. The catalyst platinum is kept at 500 – 600 °C. The heat of combustion in the presence of a gas is balanced by a reduction in electrical heating power. The power consumption serves as the signal, indicating the concentration of the gas. Thus, monitoring the effect of temperature changes at catalytic surfaces can be utilized as the gas-sensing principle.[41]

2.6 Optical Gas Sensors

Optical gas sensors play an important role in the sensing field for the measurement of chemical and biological quantities. The first optical chemical sensors were based on the measurement of changes is the absorption spectrum. At present, a large variety of optical methods are used in chemical sensors and biosensors, including ellipsometry, spectroscopy (luminescence, phosphorescence, fluorescence, Raman), inteferometry (white light interferometry, modal interferometry in optical waveguide structures (grating coupler, resonant mirror), and surface plasmon resonance (SPR). In these sensors, a desired quantity is determined by measuring the refractive index, absorbance, and fluorescence properties of the analyte molecules or a chemo-optical transducting element.[42]

2.7 Electrochemical Sensors

Chemical species reacting to an electronic conductor on ionic conductor interface exchange electric charge, resulting in an electric signal. Electrochemical gas sensors employ an electrochemical cell consisting of a casing that contains a collection of chemical reactants (electrolytes or gels) in contact with the surroundings through two terminals (an anode and a cathode) of identical composition. For gas sensors, the top of the casing has a membrane that can be permeated by the gas sample. Oxidation takes place at the anode, and reduction occurs at the cathode. A current is created as the positive ions flow to the cathode and the negative ions flow to the anode. Gases that are electrochemically reducible, such as oxygen, nitrogen oxides, and chlorine, are sensed at the cathode, while electrochemically oxidized gases, such as carbon monoxide, nitrogen dioxide, and hydrogen sulfide are sensed at the anode.[43] The output of the electrochemical cell is directly related to the concentration or partial pressure of the gaseous species. Depending on whether the output is an electromotive force (namely an open circuit voltage) or an electrical current, the electrochemical gas sensors can be classified as potentiometric or amperometric. Potentiometric measurements are performed under conditions of near-zero current. Amperometric sensors are usually operated by imposing an external cell voltage that is sufficiently high to maintain a zero-oxygen concentration at the cathode surface; therefore, the sensor current response is diffusion-controlled. Solid-state electrochemical devices are the most frequently used sensor type for the measurement of oxygen for automotive market where legislation has restricted the permitted emissions levels of carbon monoxide, hydrocarbons, and nitrogen oxides.

A potentiometric sensor based on yttria-stabilized zirconia (YSZ), together with a three-way catalyst (TWC) system, represents the most-used system for emission control at this time. The TWC system oxidizes carbon monoxide and unburned hydrocarbons and reduces nitrogen oxides. In order for the catalyst to function, the input air to fuel ratio to the engine must be maintained close to the equilibrium balance between fuel and oxygen at the so-called lambda (λ) point. The air-fuel ratio is maintained most effectively at this value by a closed-loop control system that measures the oxygen content of the exhaust gas.[44]

The foregoing discussion of various types of gas sensing technologies and their transduction principles is summarized in figure 2. Sensing material captures a molecule of vapor with a certain selectivity that induces physical change in the material because of captured molecule's chemical interaction with the material.

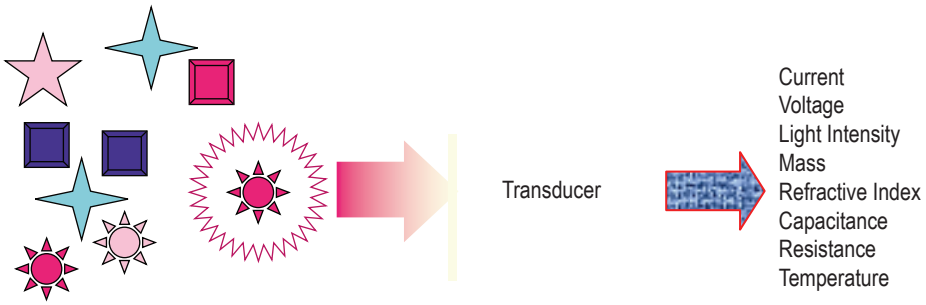

Figure 2. Molecular recognition conversion into physical signal.

3. MECHANISMS AND PRINCIPLES OF METAL OXIDE GAS SENSORS

The review of the operation of the semiconducting, metal-oxide-gas-sensing materials begins with the expounding function of the gas sensor in a qualitative manner. This is followed by the definition and description of the various sensor performance parameters and factors affecting the performance of sensors, including techniques to improve the sensor characteristics.

3.1 Working Principle

Thin films of metal oxides like ZnO, SnO_2, WO_3 etc. heated to 200 °C to 300 °C in air sensitively respond to a wide range of oxidizing and reducing analyte gases via conductivity changes. The process involved in sensing is described below:

1. Diffusion of reactants to the active region,
2. Adsorption of reactants on to active region,
3. Surface reaction,
4. Desorption of products from active region, and
5. Diffusion of products away from active region.

Diffusion of reactants to the active region depends on the ambient temperature of the measurand atmosphere, which is generally assumed to be room temperature. Once the molecules of measurand gas diffuse into the active layer, they tend to adhere to the sensing surface in a process called adsorption. Adsorption is of two types: physisorption and chemisorption. In the case of physisorption, only weak physical forces (van der Waals-type forces) bond the species to the surface. Chemisorption bonds have a re-arrangement of the electron density between the adsorbed gas and the surface. When a solid is terminated by a surface, the surface atoms are incompletely coordinated. One or two nearest neighbors are missing, and there are dangling bonds that are unsatisfied, that is, unshared with neighbors.[45] Specifically, in an ionic crystal like ZnO, both cations and anions have poor coordination. The positively charged Zn ions on the surface have an incomplete shell of negative oxide ions around them. A model rationalizing the behavior of the sensor in the measured environment originally put forward by Mark and Windischmann[46] is described below:

$$\tfrac{1}{2}O_2 + e^- \rightarrow O^-_{ads} \tag{1}$$

$$R(g) + O^-_{ads} \rightarrow RO(g) + e^- \quad , \tag{2}$$

where R (g) and RO (g) represent reducing gas and oxidized reducing gas, respectively. Oxygen adsorbs on the surface and dissociates to form O^-. An electron is extracted from the semiconductor by this O^-. This electron extraction leads to the creation of a depletion region near the surface leading to an increase in (assuming *n*-type semiconductor) resistance of the gas sensor. Figure 3 shows a three-dimensional view of the crystallite of gas-sensitive material after adsorption of oxygen.

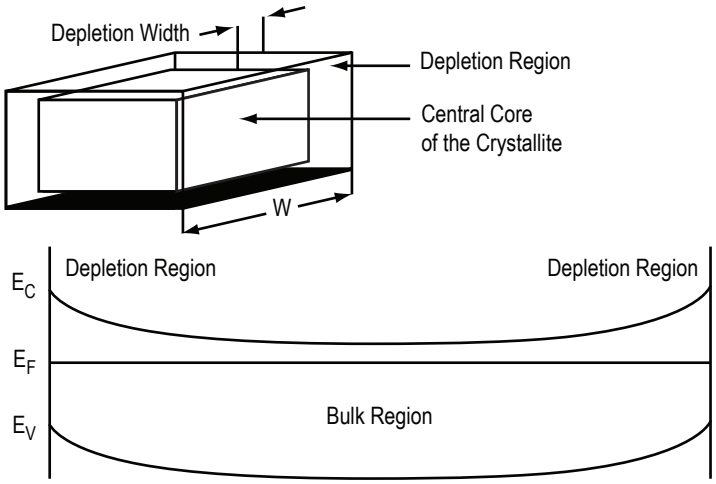

Figure 3. Three-dimensional and two-dimensional representation of the depletion region in the energy band of the crystallite in presence of atmospheric oxygen at a certain temperature.

Also detailed in the figure is the band-bending near the surface. This is attributed to the charged, double layer formation near the surface. Figure 4 shows the single-sided band bending of the semiconducting crystallite in presence of atmospheric oxygen at a certain temperature. The usual symbols E_C, E_V, and E_F represent conduction band, valance band, and Fermi level for the crystallite. The crystallite is a grain in a microstructure having finite size within thin-film or thick-film.

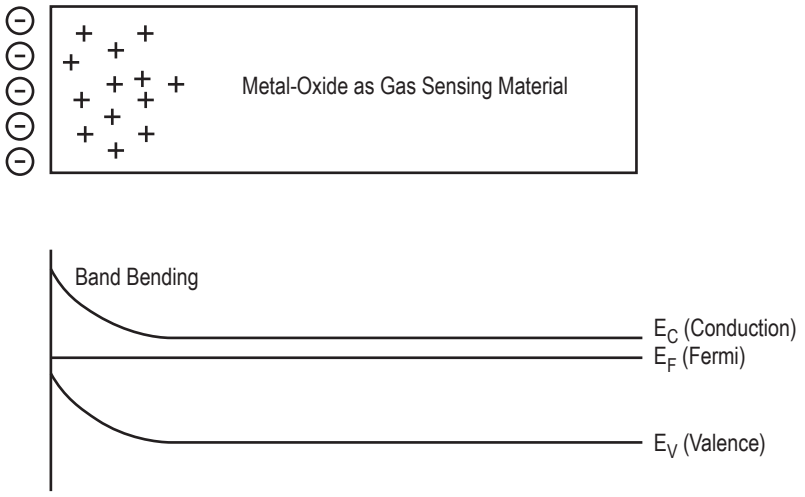

Figure 4. Distribution of charges and energy band diagram for the *n*-type metal oxide gas sensing material surface on oxygen chemisorption.

In the presence of a combustible gas like hydrogen, the gas reacts with the adsorbed O– to form water, and the electron is re-injected to the semiconductor, tending to decrease the resistance. A competition results between oxygen removing the electrons and the combustible gases restoring the electrons.[45] Since the concentration of oxygen in the measurand environment is constant, the steady-state value of the resistance depends on the concentration of the combustible gas. The competing reactions are illustrated below:

$$O_2 + 2e^- \rightarrow 2O_{ads^-} \tag{3}$$

and

$$H_2 + O_{ads^-} \rightarrow H_2O + e^- \ . \tag{4}$$

In the presence of more H_2, the density of O– reduces, leading to higher electron density in the semiconductor. Thus, the resistance of the semi-conducting film is lowered. Another model that could exist or coexist is one where the combustible gas, if chemically active, extracts lattice oxygen from the metal oxide. This results in the creation of vacancies that act as donors. The oxygen from air tends to re-oxidize the oxygen-removing donor vacancies. Thus, there is a competition between the oxygen-removing donor vacancies and the combustible gas that is producing donor vacancies. The density of donor vacancies (and hence the resistance) then depends only on the concentration of combustible gas, because oxygen pressure is constant. This is illustrated below:[45]

$$CO + M^{2+} + {O_L}^{2-} \rightarrow CO_2 + M^{2+} + 2e^- \tag{5}$$

where O_L is the lattice oxygen and M is the metal cation. Thus, two different classes of mechanisms of operation of semiconductor gas sensors can be distinguished for reducing and oxidizing analyte gases. The first class involves changes in conductance due to extraction and re-injection of electrons from the film by the surface reaction of reducing gas with adsorbed oxygen. The second involves the removal of lattice oxygen by combustible gas leading to creation of donor vacancies. The donor vacancies, in turn, inject carriers into the conduction band of the semi-conducting film leading to change in conductance.

Upon sensing of the gas by the gas sensor, adsorbed gas can either remain adsorbed on the sensor indefinitely (at low temperatures), react with the sensing material (sensor poisoning), or desorb and diffuse back into the surrounding atmosphere. Desorption refers to disengagement of a molecule or an atom from a surface. Like adsorption, desorption is also thermally activated process. When the gas desorbs and diffuses away from the sensor surface, the sensor is ready for the next measurement. The period for which the sensor is unusable is termed as dead time.

4. SENSOR PARAMETERS

4.1 Sensitivity

Sensitivity is the device characteristic of perceiving a variation in physical and/or chemical properties of the sensing material under gas exposure. This term is also used to refer either to the lowest level of chemical concentration that can be detected or to the smallest increment of concentration that can be detected in the sensing environment. The sensitivity, in the case of resistive gas sensors, is defined as the ratio of the resistance of the sample measured in air to the target gas-containing atmosphere. Sensitivity for the reducing gases is given by the following:

$$S = R_A / R_G \ , \tag{6}$$

where $R_G < R_A$, and sensitivity for the oxidizing gases is given by the following:

$$S = R_G / R_A \ , \tag{7}$$

where $R_G > R_A$ with R_G is the sensor resistance under the influence of a target gas and R_A is the sensor resistance in the reference atmosphere. Sensitivity is also calculated using the following:

$$S = \frac{R_A - R_G}{R_G} \times 100 \ , \tag{8}$$

where R_G is the sensor resistance influenced by the vapors, and R_A is the sensor resistance in the air.

4.2 Selectivity

Selectivity of the resistive gas sensors is still a major problem to be solved. It is related to the discrimination capacity of a gas-sensing device for a mixture of gases. In other words, selectivity refers to the ratio of the sensor's ability to detect what is of interest, over the sensor's ability to detect what is not of interest. Unfortunately, the selectivity of the metal oxide gas sensor is broad, responding to all reducing gases that interact with oxygen on the surface of the sensor.

In this framework, catalytic additives can lead to an improvement of the sensor activity by means of a selective promotion of a desired molecule reaction in a chosen site. Moreover, the appropriate catalytic element modifies the temperature of response of the sensing material to the desired target gas. Selectivity is often tailored and adjusted to the analyte(s) of interest by varying a wide range of parameters including dopants, grain-size, catalysts, external filters, operating temperature, and many other factors.[47]

4.3 Robustness

Robustness at the sensor level refers to the ability of the sensor to perform its function over a range of ambient conditions with humidity, temperature, etc. and over a period of time in the presence of drift and stability variations. Unfortunately, the parameters of a chemical sensor technology adjusted to improve robustness are often the same parameters that result in a decrease in sensitivity and selectivity.[48,49] For example, the most sensitive chemical sensor is often one whose reactions are totally irreversible. However, reversible reactions are desired. Design with the backing of the theory can result in a fine balance between robustness and sensitivity.

4.4 Speed of Response: Response Time

In gas detection, response time is usually defined as the time taken to achieve 90 percent of the final change in conductance, following the step-change in gas concentration at the sensor. However, sometimes 50 percent or 70 percent of the final change is also referred to as response time in literature. This is particularly the case in semiconductor metal oxide (SMO) gas sensors, because the sensors have a very fast initial response, followed by long drawn out tail before reaching the steady state values.[50]

4.5 Factors Influencing the Performance

4.5.1 Long Term Effects - Baseline Drift

Baseline refers to the conductance of the sensor in clean air. Changes over long operating times of both baseline and sensitivity are all-important in the utilization of the sensors. These determine the frequency at which the calibration check should be carried out and the frequency at which the sensors may have to be replaced. They can only be determined over long periods of time, and no method by which the process can be accelerated is valid.[50]

4.5.2 Sensor Surface Poisoning

The surface of ZnO and other oxides may become unstable because of "poisons." Sulfur in the form of H_2S is a potential poisonous gas, which can block the catalytic activity of Pd on the surface. Another dominant poison is chlorine gas. Thus, it is important in the development of sensors to be aware of other reactive gases in the measured environment.[50]

4.6 Ways to Improve Sensors

4.6.1 Use of Catalyst

Metal oxide gas sensors need a catalyst deposited on the surface of the film to accelerate the reaction and to increase the sensitivity. A catalyst is a material that increases the rate of chemical reactions without itself being changed. It does not change the free energy of the reaction but lowers the activation energy. Catalysts are supposed to, and do, impart speed of response and selectivity to gas sensors.[51] The catalytic surface reaction used for gas-sensing makes this field close to that

of heterogeneous catalysis; the only difference is that, in catalysis, one is mainly interested in the products of the reaction, whereas in gas sensing, one is interested in the reactants, as shown in the figure 5. This approach is considered relatively standard in fields such as heterogeneous catalysis, but so far, it has been applied rarely to solid-state gas sensors.

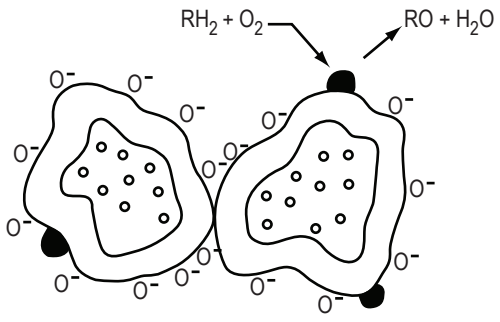

Figure 5. Illustration of catalyst effect for the nanoparticles having higher surface area acting as catalysts for reducing gas, R.[55]

The catalyst chosen influences the selectivity of sensor. Ideally, if one wants to detect a particular gas in a mixture of gases, one would like a catalyst combination that catalyzes the oxidation of the gas of interest and does not catalyze the oxidation of any other gas. Unfortunately, such ideal combinations are difficult to find.[52] The widespread applicability of semi-conducting oxides, such as SnO_2 or ZnO, as gas sensors is related both to the range of conductance variability and to the fact that they respond to both oxidizing and reducing gases.

Small amounts of noble metal additives, such as Pd or Pt, are commonly dispersed in the semiconducting oxides as activators or sensitizers to improve the gas selectivity, sensitivity, and to lower the operating temperature.[53,54] There are two ways in which the catalysts can affect the inter-granular contact region and hence affect the film resistance. One is the spillover mechanism, and the other is Fermi energy control. Catalytic theory has been proposed, since spillover and Fermi energy control have not led to a widely accepted catalyst mechanism that predicts or explains sensor behavior in different environments.[55] In spite of all the work reported, a deep analysis of the material-gas interaction and its influence on the sensor-electrical response still lacks a complete understanding the role played by the additives on the gas-sensing mechanism. A model that increases in sensitivity by using nanoparticles has been explained by activated charge carrier creation and tunneling through a potential barrier.[55]

4.6.2 Spillover Mechanism

Spillover mechanism is a well-known effect in heterogeneous catalysis and is probably most active with metal catalysts. This interaction is a chemical reaction by which additives assist the redox process of metal oxides. The term spillover refers to the process, illustrated in figure 6, where the metal catalysts dissociate the molecule; then the atom can ‘spillover’ onto the surface of the semiconductor support. At appropriate temperatures, reactants are first adsorbed on to the surface

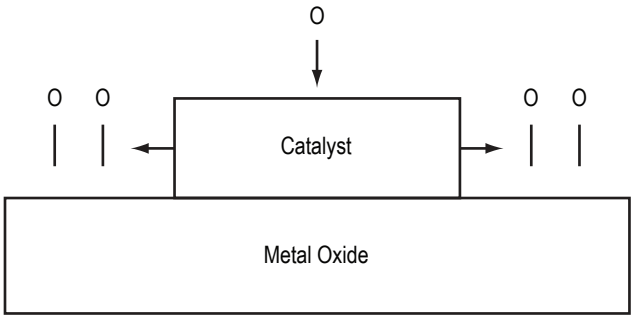

Figure 6. Schematic diagram of the spillover phenomenon; oxygen approaches the surface of the catalyst, which in turn causes the dissociation of the oxygen-gas interface.

of additive particles and then migrate to the oxide surface to react there with surface oxygen species, affecting the surface conductivity. Oxygen encroaches upon the surface of the catalyst, which in turn causes the dissociation of oxygen or gas.[56]

For the above processes to dominate the film resistance, the spilled-over species must be able to migrate to the inter-granular contact, as shown in the figure 7. Thus, for a catalyst to be effective, there must be a good dispersion of the catalysts, as shown in figure 7, so that the catalyst particles are available near all inter-granular contacts.[57] Only then can the catalysts affect the important inter-granular contact resistance.

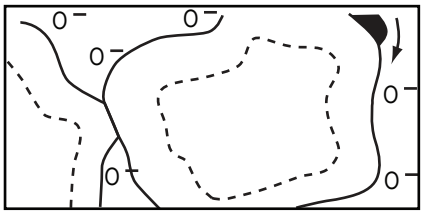

Figure 7. Illustration of spillover caused by catalyst particles on the surface of the grain of the polycrystalline particle.[57]

The inverse effect may also occur[58] when a nascent oxygen or gas atom is newly formed from a reaction on a metal oxide site. The nascent atom may migrate to a metal site and desorb into a gas molecule from there. This is called reverse spillover or the porthole effect.

4.6.3 Fermi Energy Control

The second interaction is an electronic one in which an additive interacts electronically with the metal-oxide as a sort of electron donor or acceptor. For example, changes in the work function

of the additive due to the presence of a gas will cause a change in the Schottky barrier between the metal and the oxide, and, thus, a change in conductivity. This simply means that oxygen adsorption on the catalyst removes electrons from the catalyst, and the catalyst, in turn, removes electrons from the supporting semiconductor. Figure 8 illustrates the situation with Fermi energy control. Oxygen adsorbed on the surface causes the extraction of electrons from the metal catalyst, which in turn depletes the semiconductor of the electrons.[59]

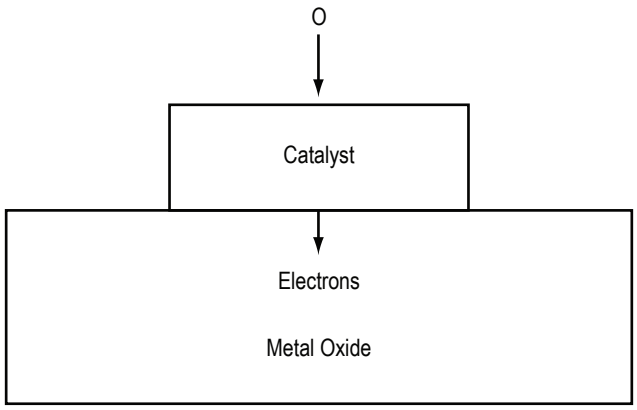

Figure 8. Schematic diagram for Fermi energy control phenomenon: oxygen adsorbed on the surface causes the extraction of electrons from the metal catalyst, which in turn depletes the semiconductor electrons.[59]

Figure 9 shows that the catalyst, by Fermi energy control, dominates the depletion of electrons from the semiconductor surface, but the poor catalyst dispersion precludes any influence on the inter-granular contact resistance. In other words, oxygen adsorbing on the catalyst removes electrons from the catalyst, and the catalyst, in turn, removes electrons from the nearby surface region of semiconductor. But if only a few catalyst particles are on each semiconductor particle, only a small portion of the semiconductor surface has a surface barrier controlled by the catalyst. Then the chances of a catalyst particle being near enough to the inter-granular contact to control its surface barrier is small. Figure 9(b) shows more desired situation where one has a good dispersion of the catalyst particles, such that the depleted regions at the surface of a metal-oxide overlap and the influence of the catalyst extends to the inter-granular contact. An adequate dispersion of the catalysts is required in order to affect effectively the grains of the semi-conducting material and serve the implied purpose of an increase in sensitivity.[56]

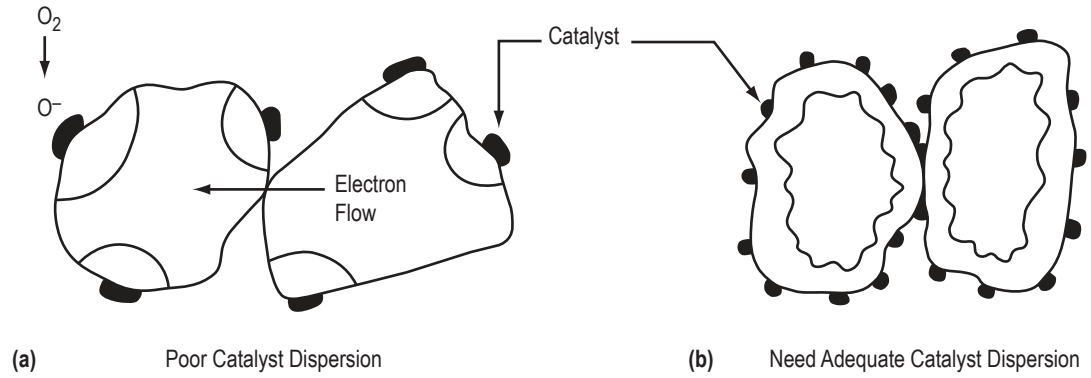

Figure 9. Schematic of the catalyst dispersion: (a) poor catalyst dispersion and (b) need adequate catalyst dispersion.

4.6.4 Grain-Size Effect

One of the important factors that affects the sensing property of semi-conducting gas sensors is the microstructure of polycrystalline element. Each crystallite of semiconductor oxide in the element has an electron depleted surface to a depth of L in air, where L is determined the by Debye length and the strength of chemisorptions. If the diameter, D, of the crystallite is comparable to $2L$, the whole crystallite is depleted of electrons, and this would cause the gas sensitivity of the element of the reducing gas to change with D. The crystallites in the gas-sensing elements are connected to the neighboring crystallites either by grain-boundary contacts or by necks. In the case of grain boundary contacts, the electrons should move across potential barrier, the height of which changes with surrounding atmosphere.

The gas sensitivity in this case is independent of the grain-size. In the case of conduction through necks, electrons move through the channel penetrating through each neck. The aperture of the channel is attenuated by the surface space charge layer. This model is related to the grain-size through the neck size. It has been discovered experimentally that the neck size X is proportional to D, with a proportionality constant of 0.8 ± 0.1. For $D >> 2L$, conduction of electrons in the sensing element is dominated by conduction through grain boundary contacts (grain boundary control).[60] For $D > 2L$, neck control forms the primary mechanism of conductivity modulation (neck control). For $D < 2L$, the electrical resistance of the grains dominates the whole resistance of the sensor and thus sensitivity is controlled by the grains themselves (grain control). The grain-size effects are pictorially depicted in figures 10 and 11.[60]

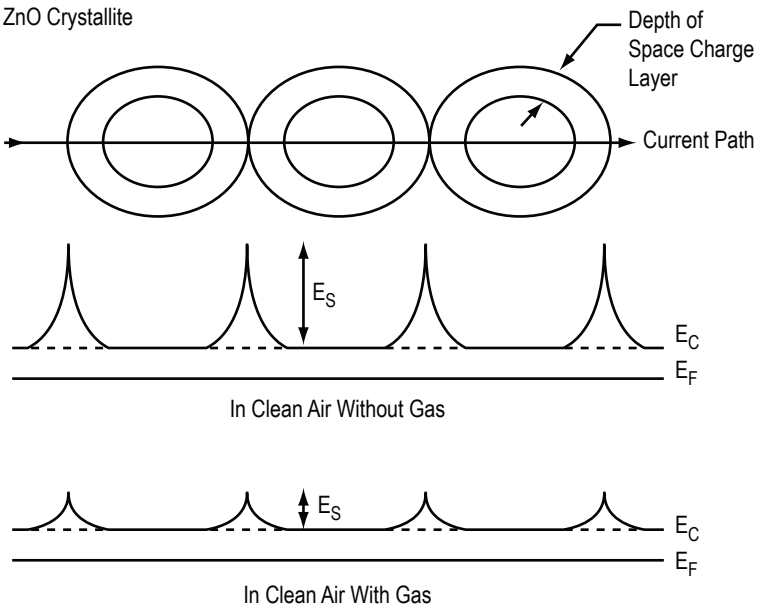

Figure 10. Potential barriers for the crystallite diameter of the sensing film is more than twice the space charge layer depth (width). The change of the potential barrier, E_S, is shown with and without the presence of the gas. E_F is the Fermi level and E_C is the conduction band edge.[60]

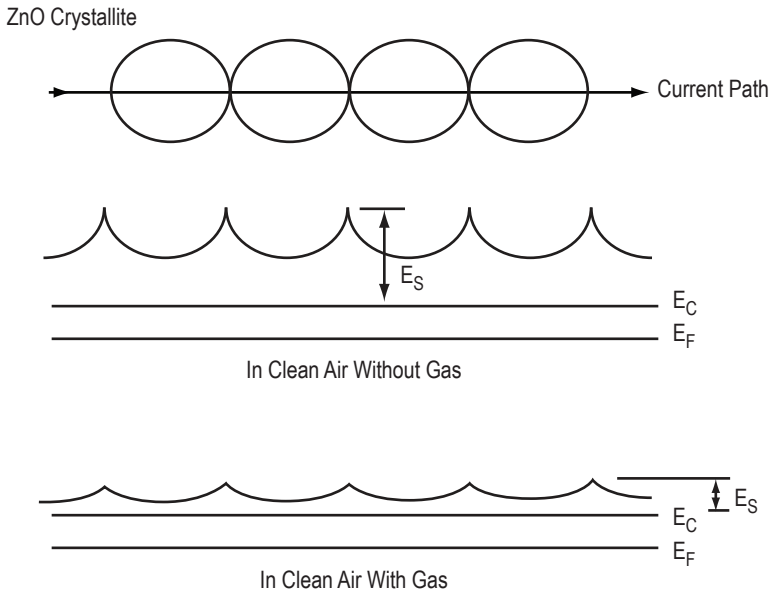

Figure 11. The crystallite size of sensing film is higher than the depletion width resulting in incomplete depletion of grain: energy barrier for electron in presence and also in absence of gas.

4.6.5 Thickness Dependence

Thin- and thick-film sensing layers differ not only in their thickness, but also in their microstructures and can thus lead to rather different transducer functions.[61] The sensitivity of the layers depends strongly on the layer thickness. If the thickness of the electron depleted surface thickness is about the size of a film, high gas-sensitivity can be expected. Thus, sensitivity of the metal oxide sensor is directly influenced by the size of the oxygen-induced depletion layer at the film surface relative to the thickness of the bulk semiconductor. In general, when the depletion width equals the film thickness, more sensitivity is expected.

Figure 12(a) shows the depletion region in the atmosphere ambient whereas, Figure 12(b) shows the reduction in the depletion depth upon being exposed to the reducing gas. When the depletion depth is more or less equal to the thickness of sensing film, the resistance will be high and hence contribute to the higher sensitivity. However, it has been pointed out by Becker et al.[62] that the columnar growth of a gas-sensitive film leads to the thickness-independent gas sensitivity of the sensor. It has also been shown that the thickness of the sensitive layer does play a role in determining the sensitivity of the sensor for different gases.[48] The thin SnO_2 layer, (thickness 50-300 nm) mainly responds to the oxidizing gases, such as ozone (O_3) and NO_2, whereas thick films (thickness 15-80 μm) respond to reducing gases, like CO and CH_4. However, upon reducing the temperature of the sensor, the thick film showed a significant response to oxidizing gases. This behavior can be explained with the diffusion reaction model. A model for the sensing mechanism in thick-film is presented in reference.[48]

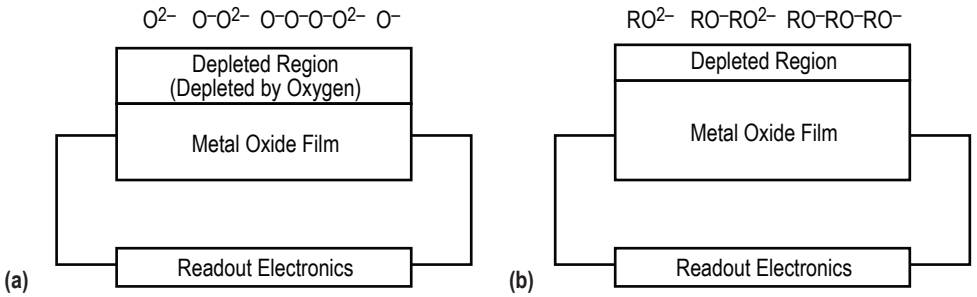

Figure 12. Sensitivity dependence on the depletion layer in the metal oxide: (a) adsorption of the atmospheric oxygen on the surface of sensing film resulting in the increase in the resistance of the film and (b) reduction in depletion area upon exposure to the reducing gas, causing a decrease in the resistance of the film.[60]

4.6.6 Temperature Modulation

The temperature of the sensor surface is one of the most important parameters. First, adsorption and desorption are temperature-activated processes. Thus, dynamic properties of the sensors viz. response time, recovery, etc. depend on the temperature. The surface coverage, co-adsorption, chemical decomposition or other reactions are also temperature dependent,

resulting in different static characteristics at different temperatures. On the other hand, temperature has an effect on the physical properties of the semiconductor sensor material, such as charge carrier concentration, Debye length, work function, etc. The optimum range of temperature for an effective sensor response corresponds to where the material is able to reduce catalytically or oxidize the target gas, simultaneously changing the electrical properties of the sensor material. The rate of reaction depends on the exact reducing agent under study.

With a given reducing agent, there is peak in the sensitivity. If the temperature is too low, the rate of reaction is too slow to give a high sensitivity, but if the temperature is too high, the overall oxidation reaction proceeds so rapidly that the concentrations of reducing agent at the surface becomes diffusion-limited, and concentration seen by the sensor approach zero.[57] At such temperatures, the whole target gas concentration reaching the material surface could be reduced/oxidized without producing a perceptible electrical change on the metal-oxide material. The sensitivity again is low. However, temperature should be high enough to allow gas reaction on the material surface. The operating temperature is chosen empirically to provide the highest sensitivity to the determinate gases. So, a clear understanding of the relation between the sensing material, catalytic properties, and the sensor electrical response is indispensable to understand the whole gas-sensing mechanism.

For each sensor-gas combination, an optimum temperature between these limits must be used. When higher degrees of selectivity are needed, sensor arrays (sometimes trained "electronic noses") having the different responses of various sensors are used for identifying the gaseous species by pattern matching. With such sensor array, the lack of selectivity of the single metal-oxide gas sensor can be overcome by processing the signals of the same kind of sensor devices at different operating temperatures or of the device using different materials at the same temperature.[63–65]

4.6.7 Filters for Selectivity

The use of filters forms another approach to improve the selectivity of gas sensors. These filters either consume gases that one does not wish to pass to the gas sensor or permit the passage of selected gases to the sensor. Their use is, to a great extent, empirical. For example, Ogawa et al.[66] claim that ultra-fine SnO_2 rejects methanol. Carbon cloth and low porosity materials are used to prevent highly reactive or large molecules from reaching the sensor. Silica can be used to increase hydrogen sensitivity, as hydrogen passes more freely through the silica surface layer. Similarly Teflon® is helpful in stopping H_2O reaching the sensor material and zirconia (ZrO_2) can be used at high temperature to pass oxygen.[1]

4.6.8 AC and DC Measurements

The sensor's resistance change is the best-known sensor output signal and is, in most cases, determined at constant operation temperature and by DC measurement. The inherently noisy behavior of the resistor—1/f noise also known as flicker noise—in the DC resistance measurements can often approach the desired sensitivity threshold of the sensor. AC resistance measurements are one way to overcome prohibitive 1/f noise, but they incur more complex measurement electronics and calibration reproducibility issues. AC measurements are more frequently used in the form of

impedance spectroscopy[12,13] at the modeling level attributing to the operative mechanisms. Weimar and Gopel[56] reported that sensitivity and selectivity of the gas sensors can be improved by applying both DC and AC measurements. It has been demonstrated that the use of different contact arrangements and monitoring conduction at different frequencies make it possible to discriminate among the gases.

5. MICROSTRUCTURED METAL OXIDE CHEMICAL SENSORS

Gas sensors based on wide-band semiconductor metal oxides are playing an important role in the detection of toxic pollutants (CO, H_2S, NO_x, SO_2, etc.) and combustible gases (H_2, CH_4 and flammable organic vapors, etc.). Metal oxides, such as SnO_2, ZnO, TiO_2, WO_3, Ga_2O_3, etc., have been examined for gas sensing applications and for control of industrial processes. SnO_2 is the most extensively studied material among other studied metal oxides.[1–7] Various techniques have been used to improve the sensitivity and selectivity of these sensors. As a matter of fact, a large part of the literature deals with characterization of sensors employing different forms of oxides, the effect of catalytic or other additives or ion implantation, the use of masks and filters to improve selectivity, and temperature programming techniques etc.[1–14] However, a lack of consistency in sensor properties has been a major problem associated with various techniques used for the fabrication of sensors. Bulk, thick, and thin films of SnO_2 have been used in the fabrication of gas sensors. Thin-film sensors are of great interest because of the relatively small geometry, low power consumption, and sharp sensing effect, etc. A sensor having a thin film of fewer than a few hundred nanometers has a reasonably good sensitivity, but usually shows poor stability due to weak mechanical strength. The dispersions of dopants that enhance the sensitivity over thin-film is not as satisfactory as those for thick-film or bulk type sensors.[15–17] For thick-film or bulk-type sensors, dopants (or additives) are usually mixed homogeneously with the powder precursors.

6. DEVELOPMENT OF THICK-FILM BINARY OXIDE SENSOR MATERIALS AT ALABAMA A&M UNIVERSITY

Recently, it has been reported that composite sensors incorporating differing proportions of SnO_2 and ZnO exhibit higher sensitivity over a range of organic vapors.[8] Most importantly, the composite sensors have been shown to have a significantly higher sensitivity than sensors fabricated from SnO_2 or ZnO, when operated under identical experimental conditions. It has been proposed that an increase in sensitivity is due to synergistic effects: complementary catalytic activity,[10] the formation of hetro-junctions, and changes in microstructure on sintering.[11]

The aim of the investigation at AAMU is to fabricate thick-film sensors of binary mixtures of oxides: SnO_2-ZnO, SnO_2-In_2O_3, and SnO_2-WO_3 and investigate their response, such as sensitivity and response time, to 2-isopropanol. Experimenters performed the study to predict the detection capability of these sensors for different concentrations.[12]

6.1 Gas Sensor Fabrication

The schematic design of the in-house fabricated screen-printing system is illustrated in figure 13. It consists of a base plate on which a vacuum chuck/substrate holder is placed at a predetermined location. The screen is placed close to the substrate, and ink/paste is placed on top of the screen. A soft rubber squeegee is moved across the screen that drives the paste in front of it and down through the unplugged areas of the screen onto the surface of a substrate. The screen is lifted off, leaving a patterned deposit of paste on the substrate, which is then dried and sintered to form the thick film.

Sensors were fabricated by thick-film technology (TFT) on an alumina substrate. SnO_2 powder (99.99 percent metals basis, Alpha Aesar), WO_3 powder (99.8 percent metals basis Alpha Aesar), ZnO powder (99.9 percent minimum –325 mesh powder Alpha Aesar), and In_2O_3 powder (99.99 percent metals basis Alpha Aesar) were used in the fabrication of the sensor materials. Composites produced were based on 75:25 (wt percent) SnO_2-WO_3 (TTO), 75:25 (wt percent) SnO_2-ZnO (TZO), and 75:25 (wt percent) SnO_2-In_2O_3 (TIO). In each case, oxide mixtures were grounded and milled. To prepare the ink-paste for the screen-printing, a commercially available terpineol-based vehicle ESL 449 and an active mixture were blended. The paste was then applied onto the ultrasonically cleaned alumina (Al_2O_3) substrate using screen-printing machine. The design of the sensor fabricated is shown in figure 14, and the complete process is illustrated in figure 15.

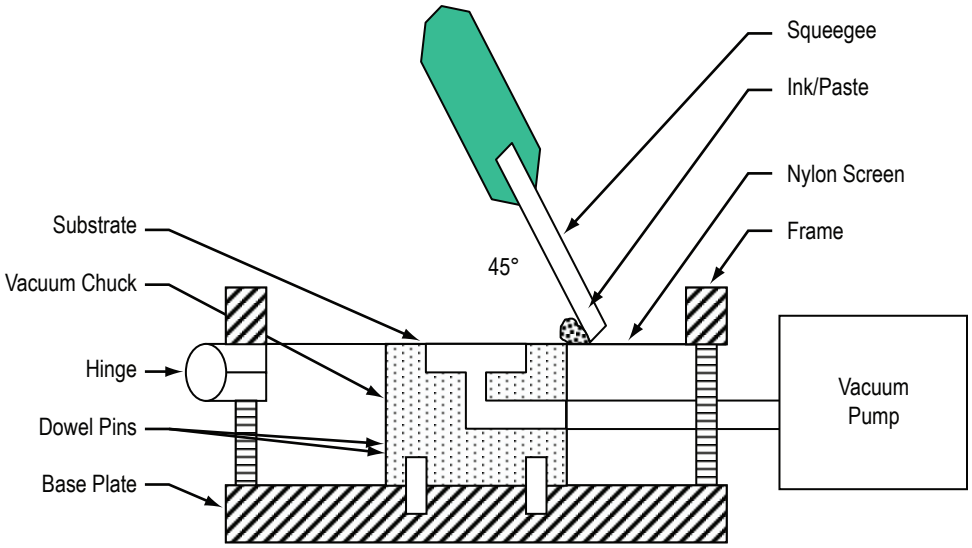

Figure 13. The illustrated design of a screen-printing system developed at AAMU.

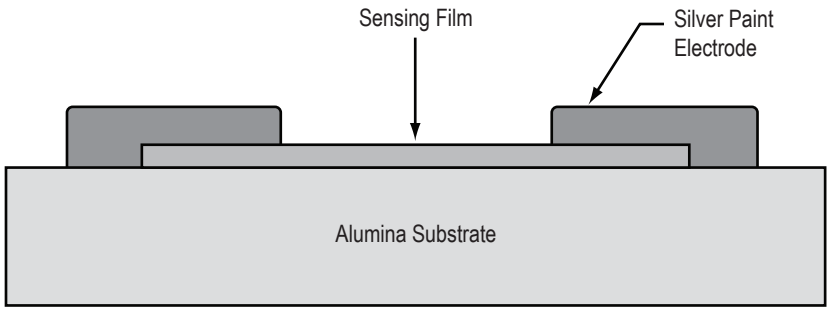

Figure 14. Cross-section of a sensor fabricated using an alumina substrate.

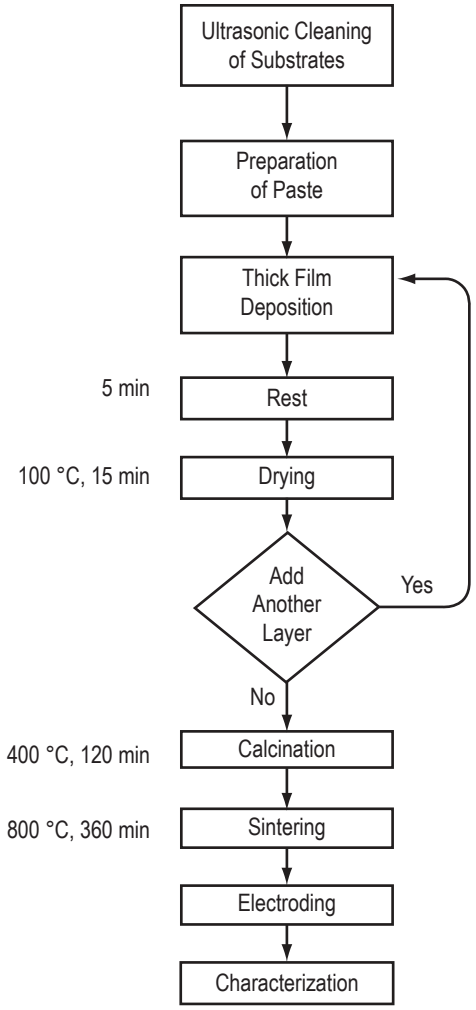

Figure 15. Thick-film transfer sensor fabrication (process) parameters developed at AAMU.

6.1.1 Furnace Heat Treatment

All samples were heat treated in a Neytech™ QeX Programmable Laboratory Bench Top High Temperature Vacuum Furnace model 94-94-400 as shown in figure 16. The furnace has a temperature accuracy of ± 3 °C at steady rate with a maximum temperature of 1200 °C. The furnace operates on a voltage range of 100 to 120 VAC power. Muffle temperature uniformity is rated at +/– 5 °C, also at steady rate. Interior muffle dimensions are 6.3 cm high by 10 cm in diameter. Distance from the door insulator to muffle when it is open is 15 cm. This particular model furnace has a built-in RS-232 port, which connects to a PC COM port via a null modem cable and runs with a proprietary NeyTech Windows® program. Other ports located on the rear of the unit are vacuum inlet, exhaust port, and pressure port. The vacuum inlet allows an operator to hook up the furnace to a vacuum pump; however, this option was not utilized because, from previous research, it was evident that ambient pressure would be sufficient for the experiments.

Figure 16. Furnace set-up designed and installed at AAMU.

Samples are loaded onto the door insulator of the furnace and then the muffle is automatically lowered. Figure 17 plots the heat treatment process. Initially the furnace is heated from ambient temperature at a ramping rate of +2 °C/min to a calcination temperature plateau of 400 °C and held for two hours. By definition, this heat treatment step allows volatiles to escape. The furnace was then heated from 400 °C at a ramping rate of +2 °C/min to a sintering temperature plateau of 800 °C and held for 6 hours. Again by definition, this heat treatment step is a ceramic process in which a material is heated to somewhere below the melting point until the particles begin to adhere to each other. The furnace was then cooled down from 800 °C at a ramping rate of –2 °C/min to ambient temperature.

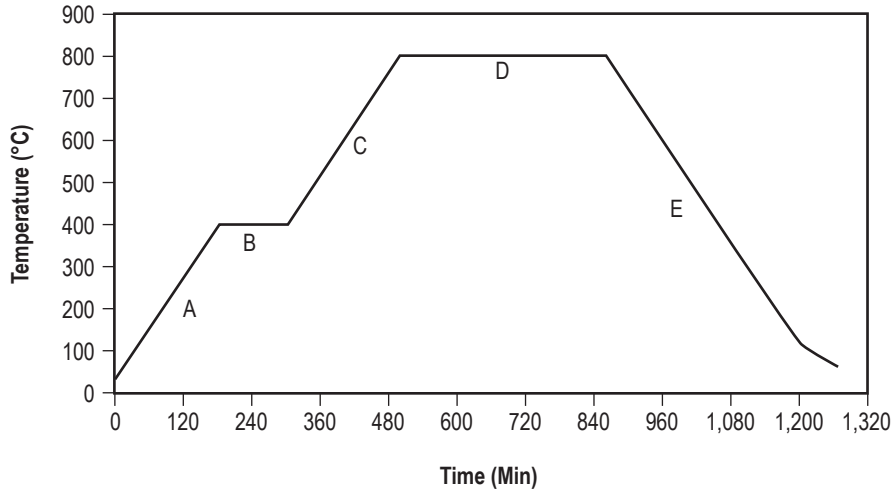

Figure 17. The heating profile: Region A represents +2 °C/min ramp rate, Region B represents calcination plateau, Region C represents +2 °C/min ramp rate, Region D represents sintering plateau, and Region E represents –2 °C/min cooling ramp rate.

6.1.2 Sensor Testing System

Resistance measurements of alumina substrate samples were made in the vapor detection test system as seen in the diagram shown in figure 18. This apparatus consists of a plexiglass box, a Keithley® 617 electrometer, a Cole-Parmer® temperature controller, a power supply, a Gateway® PC, and National Instruments® LabVIEW™ for Windows version 7.1. The vapor chamber is a plexiglass box with an internal volume of 5.2 liters. The lid was fabricated out of plexiglass and has the following attributes (figure 19). A handle was fastened to the lid for easy lid removal, which also facilitated an easy method for sample exchange. A membrane for accepting the needle of a syringe was added by drilling two holes of which one is a through-hole, and the other leaves a rim of approximately 2 mm × 2 mm.

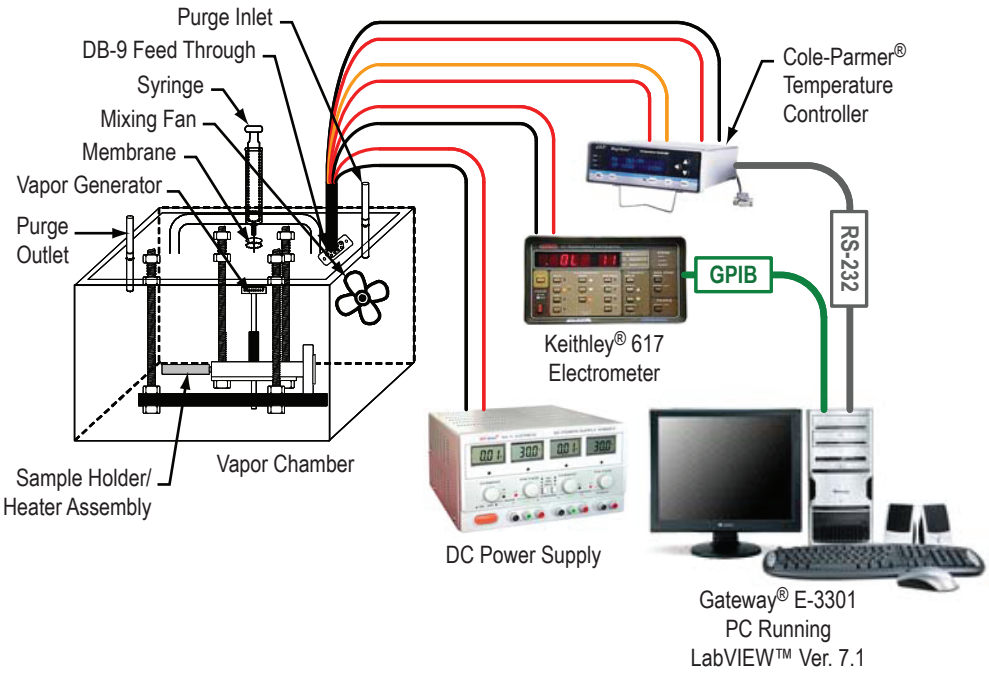

Figure 18. Organic vapor sensing system designed and developed at AAMU.

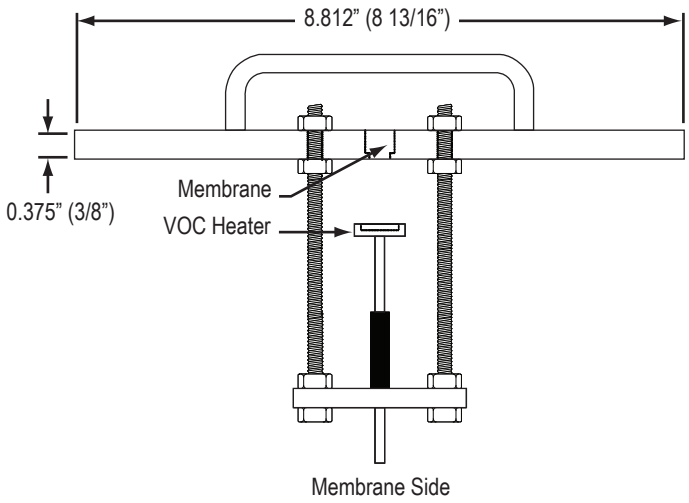

Figure 19. Back-side view of the vapor chamber lid showing vapor generator and membrane port.

Cellophane tape was placed over the bottom of the hole, and RTV was poured in and allowed to cure. Cellophane tape was removed from the bottom of the filled-in hole and another piece was affixed to the top of the hole. A vapor-generating assembly was fabricated from a semiconductor heating source that had a square, open, shallow box on one end with a hollow shaft mechanically connected as in figure 19. Heater wire was wrapped around this hollow shaft so that any liquid that touched the square, shallow box would be instantaneously vaporized. This assembly was mounted on a nylon shelf, which was suspended from the lid with all thread. This assembly was oriented directly beneath the membrane with the shallow square box being approximately 2 cm away. Figure 20 shows a left side view of the lid design with the vapor generator and sample holder. A sample holder was fashioned from a soldering iron as seen in figure 21. A rectangular piece of aluminum was machined and a hole was bored in the center of one edge to fit over the tip portion of the soldering iron and a second hole was drilled and taped for a set screw. This hole is perpendicular to the first hole. The sample holder/soldering iron assembly was then attached to a nylon plate which was suspended from the lid with 8-32 threaded screw. Two c-clamps for holding each sample to the fixture were fabricated from Teflon and a hole on one side was drilled and tapped for a brass machine screw that had the dual purpose of holding down the sample and passing electrical signals. Signals and power were passed through the lid with a DB-9 female connector. Signals included sources from the sample and a Type K thermocouple that was used as feedback to the temperature controller for heating the sample holder. Power included the heater wire for the sample holder and the vapor generating assembly. Signal from the sample was measured by the Keithley 617 electrometer. Power lines from the sample heater and the Type K thermocouple, were connected to the Cole-Parmer Digi-Sense™ temperature controller. Power lines from the vapor generator were connected to a power supply. The voltage was set to 4 V_{DC}. Additionally, there was a purge inlet port and a purge outlet port. Each was made from 0.25" ID stainless steel tubing of approximately 3 inches in length. Holes were drilled in the vapor chamber lid and each piece of tubing was pressed into place. A top view of the vapor chamber lid design can be seen in figure 21. Figure 22 illustrates the front view of the vapor chamber. Figure 23 shows photograph of the vapor testing system with complete instrumentation and figure 24 shows the vapor chamber.

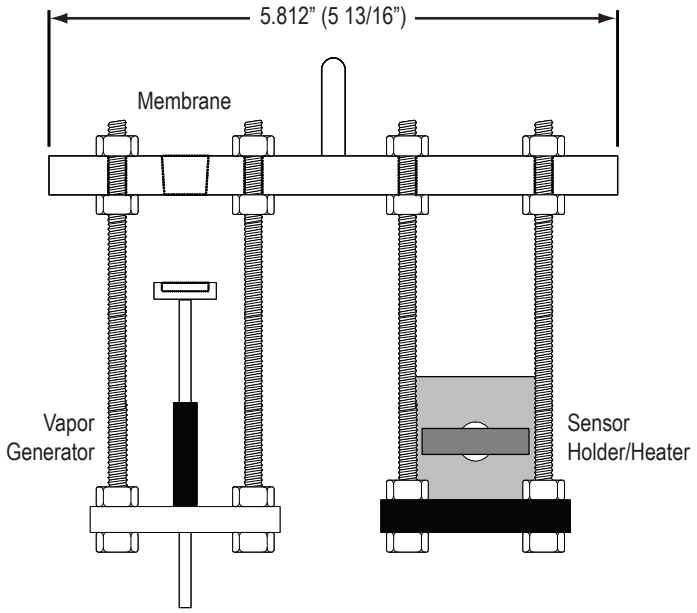

Figure 20. Inside schematic illustration of vapor chamber lid with organic vapor generator and sample holder-heater assembly.

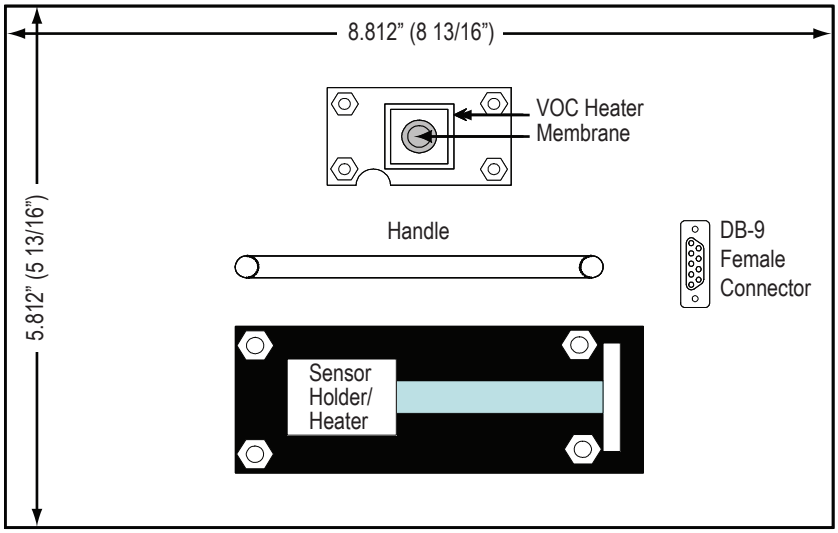

Figure 21. Top view of the vapor chamber lid with vapor generator at the top, handle in the middle, sample holder on the bottom, and DB-9 connector to the right.

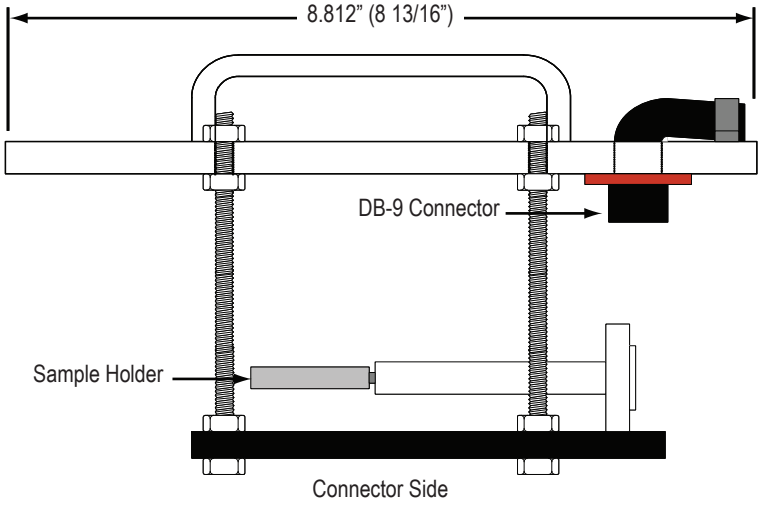

Figure 22. Front view of the vapor chamber lid with the sample holder/heater assembly and DB-9 connector.

Figure 23. Photographic view of the set-up of the vapor testing station.

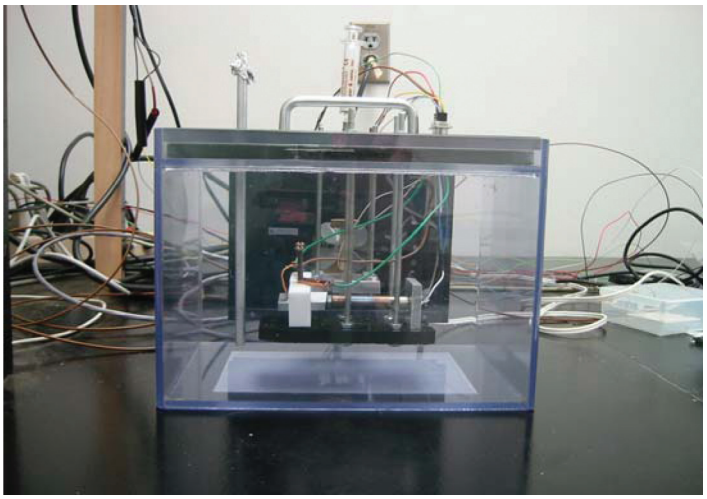

Figure 24. A close-up photograph of the vapor chamber.

6.2 Characterization of Binary Thick-Films Deposited onto Alumina Substrate

Recently, it has been reported that composite sensors incorporating differing proportions of SnO_2 and ZnO exhibits higher sensitivity over a range of organic vapors.[8] Most importantly, the composite sensors have been shown to have a significantly higher sensitivity than sensors fabricated from tin dioxide or zinc oxide, when operated under identical experimental conditions. It has been proposed that an increase in sensitivity is due to the synergistic effects: complementary catalytic activity,[9] formation of hetro-junctions, and changes in microstructure on sintering.[10]

The response time was calculated as a function of 1σ of initial output from final output resistance. The term 1σ is obtained by calculating 68.2 percent of the difference between the initial and final outputs. Then, the difference between the times of the corresponding initial and 1σ outputs is taken. The protocol of testing the vapors was as follows:

1. The sensor to be tested was mounted on the sample holder in the chamber and heated to an operating temperature of 140 °C. The sensor was allowed to thermally soak for 12 hours prior to testing.

2. The data acquisition program was initiated, and the sensor was monitored until a steady baseline resistance was attained.

3. A test liquid was injected onto the vapor generator (heater assembly) in order to convert it directly into a vapor. The response was monitored until value of the resistance is constant and steady; then an additional amount of IPA is injected into the chamber.

Three SEM micrographs of the composite oxides are depicted in figures 25 through 27. The micrographs clearly show that the structure of the active layer is homogeneous and porous except for TZO composite film (figure 25). The TZO active layer seems to be rougher than other two. To study the sensitivity of each sample, we plotted the sensitivity value against the vapor concentration. Figure 28 (a, b, and c) shows the response curve of composite oxides sensors for different concentration of isopropanol vapors. The resistance decreases on increasing the concentration in a linear manner. However, some noise was observed for TZO sensor material. Figure 29 shows the concentration of injected specie and respective sensitivity of composites oxides sensor operated at 140 °C. There is a slight increase of sensitivity with the increase of injected concentration of vapors. The sensor fabricated with SnO_2-WO_3 (TTO) composite shows the highest sensitivity for isopropanol, even at 20 ppm level among the other two sensors investigated. The sensitivity reaches saturation at about 100 ppm. At a fixed surface area, a low gas concentration implies a small surface of gas molecules. An increase in vapor concentration raises the surface coverage, eventually leading to a saturation level, thus determining the upper detection limit. Figure 30 shows the response time of composites oxides to 20 ppm isopropanol vapors.

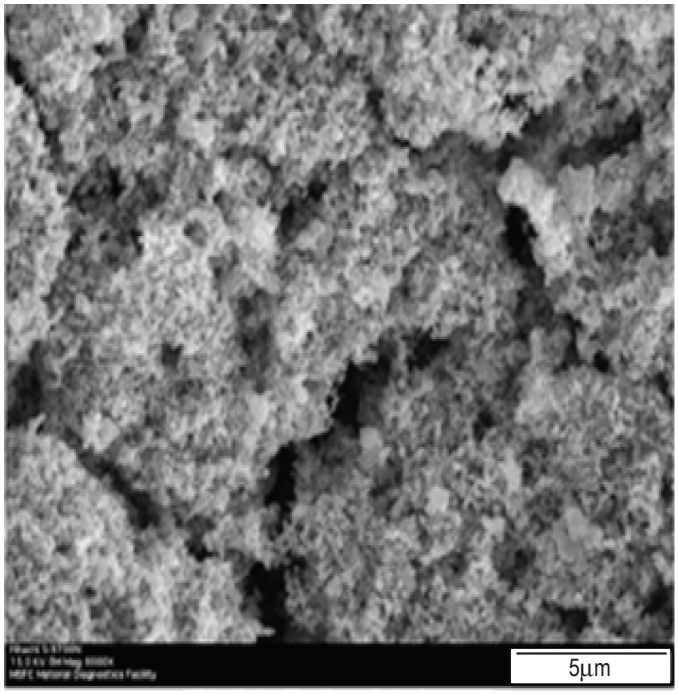

SNO2_ZnO_c04_6kx.tif

Figure 25. SEM micrograph of the surface of the TZO-sensing layer.

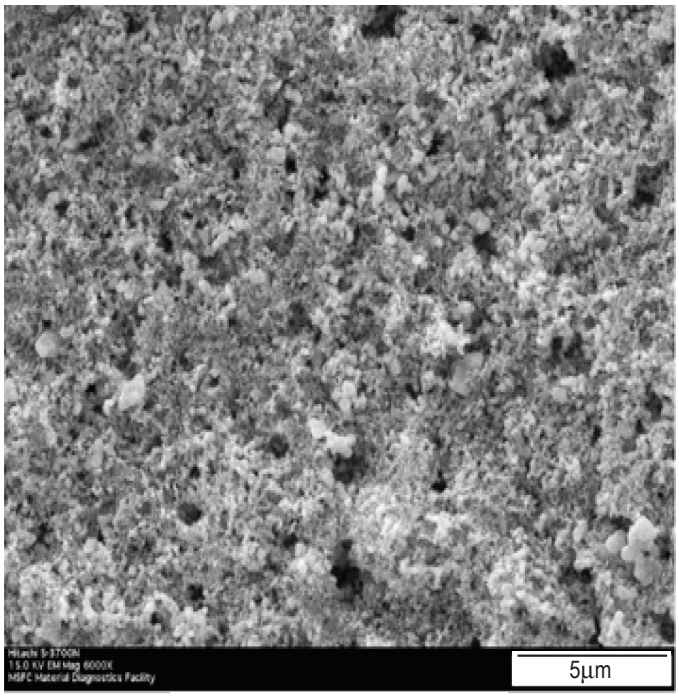

SNO2_In2O3_c04_6kx.tif

Figure 26. SEM micrograph of the surface of the TIO-sensing layer.

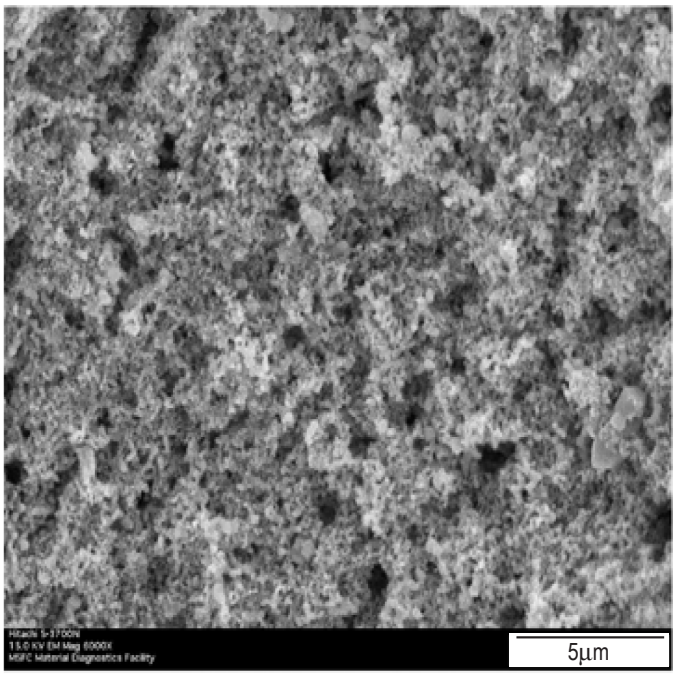

SNO2_WO3_B_c04_6kx.tif

Figure 27. SEM micrograph of the surface of the TTO-sensing layer.

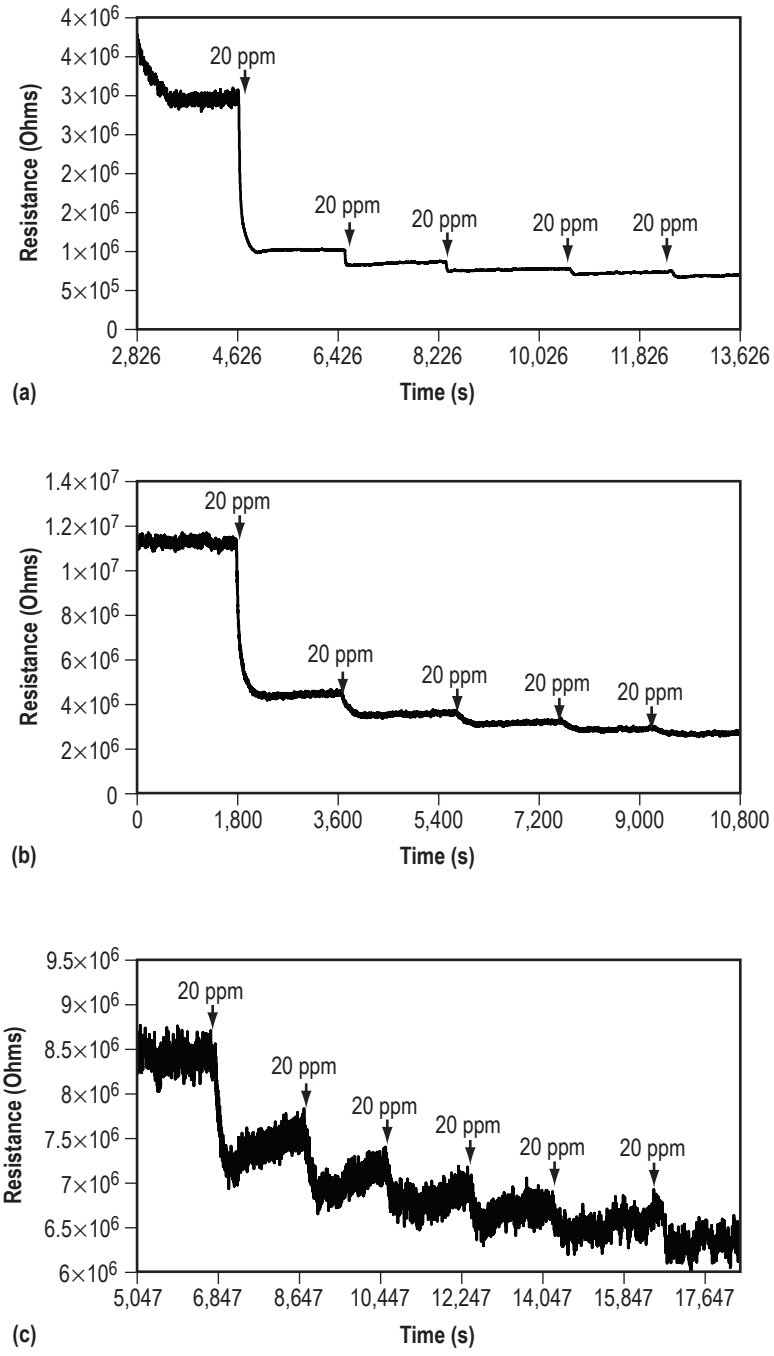

Figure 28. Response curve for (a) TTO, (b) TZO, and (c) TIO sensing materials operating at 140 °C to successive injections resulting in increased concentrations of isopropanol.

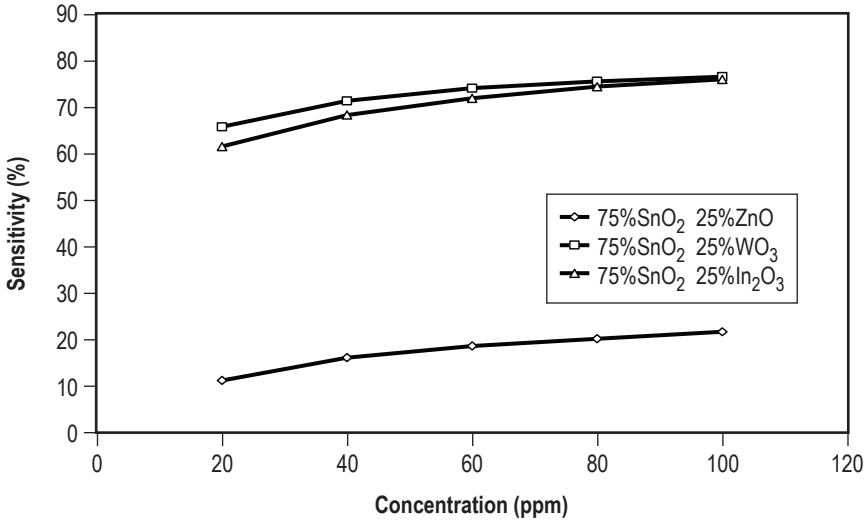

Figure 29. Sensitivity of the composite oxides of isopropanol vapor at 140 °C.

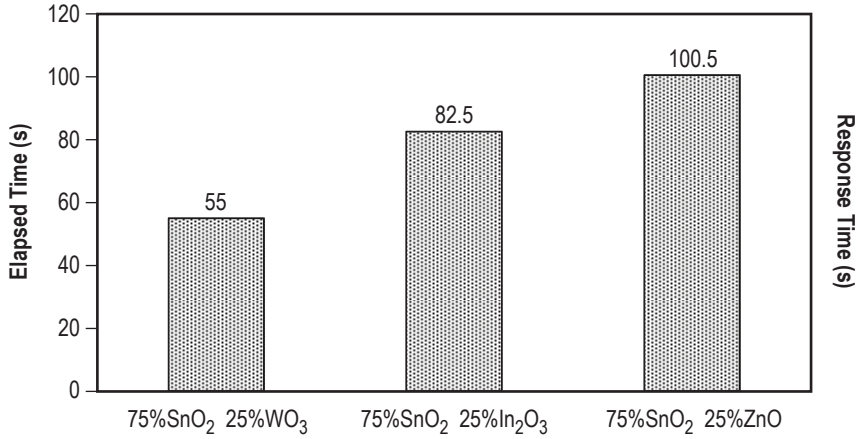

Figure 30. Response time for the composite oxides at 20 ppm isopropanol vapor.

6.3 Proposed Gas-Sensing Mechanism

The proposed gas sensing mechanism is based on change of resistance of the oxides in the sensing layer. The oxygen absorbed on the surface of the materials influences the conductance of the oxide-based sensor. The adsorbed oxygen depends mainly on the type of the materials, particularly on their chemical reaction with the gas. A chemical reaction (reduction or oxidation) between the gas and the sensing layer causes electrical conductivity of the p-type semiconductor material to increase (decrease) when oxidizing (or reducing) gases are absorbed on the surface, while the opposite occurs for the n-type materials. It has been reported that there is a sizable amount of adsorbed O_{ad} on the SnO_2-ZnO surface at room temperature.[71] The sensing property is defined by a chemical reaction which changes the concentration of electrons in the oxide surface layer. Chemisorption

will modify the defect states of the oxide's surface layer because the working temperature of SnO_2-ZnO-based NO_2 sensor is usually lower than that of bulk-conduction-based gas sensor structure.[72]

Another important issue is the particle size: the smaller the grain, the larger the specific surface area, which results in greater adsorption and higher sensitivity.[73,74] A number of adsorbed species are determined by the surface morphology of the films. Candidate materials for gas-sensing, such as ZnO, SnO_2, and tungsten oxide have non-stoichiometric structures; therefore, free electrons originating from oxygen vacancies can contribute to conductivity (n-type). In an n-type metal oxide semiconductor conduction electrons (e^-) come primarily from the point defects via O vacancies and interstitial Sn atoms,[75] and play a major role in the gas sensing operation[8,76] which is the combination of two adsorption reactions. First, the sensitizing reaction of some reactants gases adsorbed as a result of surface contact with SnO_2-MO (where M = Zn or W or Zn) and thereby forming the Schottky (rectifying) contact. This results in a change of electrical resistance of these materials indicating the presence of gas vapors. Second, the surface detection is done with the participation of oxygen, which can be present in molecular (O_2^-) or atomic (O^-) form to reduce the resistance of the SnO_2-MO layer. The reaction sequences on the IPA (CH_3-CHOH-CH_3) can be written in these steps with physical and chemical adsorption.

Step I for sensitizing reaction:

$$O_2(\text{gas}) + 2e^- \rightarrow 2O^- + \Delta H_1 \tag{9}$$

Step II for detection reaction:

$$(CH_3)_2CHOH + O^- + \Delta H_2 \rightarrow e^- + CH_3COCH_3 + H_2O + \Delta H_3 \tag{10}$$

Step III for net equilibrium reaction having addition of equations (1) and (2):

$$O_2 + 2(CH_3)_2CHOH \rightarrow 2CH_3COCH_3 + 2H_2O + \Delta H_4 \tag{11}$$

However, there are no obvious differences in the microstructure of the composites films investigated, except SnO_2-ZnO (TZO) in which coagulation of particles is observed in certain regions. In order to seek an explanation for changes in sensor response, pore size distributions have to be measured. A decrease in the number of pores is likely to be responsible for the decrease in sensor response.[77] Highly porous thick film sensors have increased sensitivity and longer response times.[78] At the same time the observed changes in sensitivity of composites oxide sensor elements may be attributed to porosity, particle size variation, and catalytic effects of tungsten, zinc, and indium. Further study is needed to resolve possible response mechanisms, i.e., change in sensor response of metal oxide thick films because of the conduction mechanism.

7. AC SMALL-SIGNAL RESPONSE OF THE SNO_2 THICK-FILM DEPOSITED ONTO ALUMINA SUBSTRATE

Figure 31 shows the impedance plot of the AC small signal electrical data along with the simulated data. The simulated data are generated using the Cole-Cole equation[67–70] of the form:

$$Z^*(\omega) = Z_\infty + \frac{(Z_S - Z_\infty)}{1 + (j\omega\tau_0)^{(1-\alpha)}} = Z' + jZ'' \quad , \tag{12}$$

where $Z_S = Z_{DC} = Z_{dc}$ implying resistance at the DC condition as $f \rightarrow$ low frequency value approaching 0 Hz (as in ideal situation); Z_∞ is the resistance at the high frequency limit, $\Delta Z = Z_{dc} - Z_\infty = Z_S - Z_\infty$, τ is the relaxation time, Z' is the real part, and Z'' is the imaginary part of Z^* with $j = \sqrt{(-1)}$. The exponent parameter α signifies finite value, ranging between 0 and 1 for the non-ideal behavior known as the Cole-Cole response.

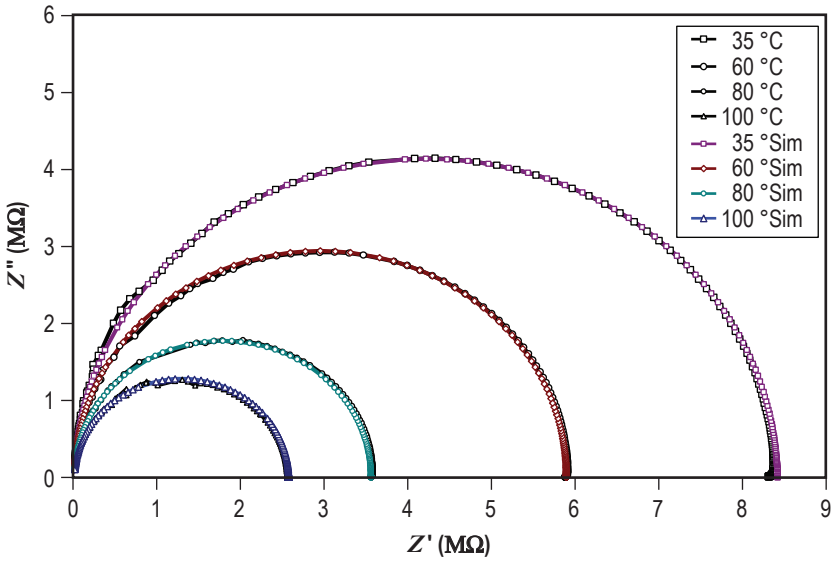

Figure 31. Impedance plot of the thick-film containing SnO_2 with 0.5 percent Bi_2O_3 as modifier deposited on the alumina substrate.

For $\alpha \rightarrow 0$, the Cole-Cole equation achieves ideal Debye response[67–70] that is derived from the admittance expression in the parallel R-C (resistance-capacitance) circuit form. The impedance of this parallel R-C circuit form essentially reflects the combination of the series resistance and series reactance containing the series capacitance obtained via impedance plot.

The simulated impedance data are generated from the Cole-Cole equation in (12). Thus, the experimental and the simulated curves are overlapping each other for the level of accuracy of the semicircular behavior. Each experimental semicircle contains a simplified equivalent circuit, representing an intercept on the left-side at high-frequencies of the semicircular relaxation on the x-axis. This intercept may be termed as the left-intercept. The ordinate (y-axis) and abscissa (x-axis) must have the same plotting scale so that the semicircular relaxation in the complex plane can be clearly seen. This means that the magnitude of each unit grid (or graphical segment) in length on the ordinate and the abscissa must be equal. A semicircle whose center lies on the x-axis is defined as a Debye or Debye-like relaxation, which gives $\alpha \rightarrow 0$. The transformation from impedance to admittance or vice versa is straightforward and only superbly meaningful for the Debye relaxation. For a non-Debye relaxation, the center of the semicircle lies below the x-axis that gives the Cole-Cole response in the form of equation (12). A non-Debye relaxation gives rise to a depression angle (θ) measured from the point at the left-intercept to the center of the semicircle below the x-axis. This depression angle becomes a measure of the depression parameter, α where $\alpha = \theta/\pi$. The value of α depends on the idealized Debye or extreme non-Debye response of a semicircular relaxation. Thus, a Debye-like behavior can be achieved as $\theta \rightarrow 0°$ [$\alpha \rightarrow 0$] and an extreme non-Debye response can be visualized with $\theta \rightarrow 90°$ [$\alpha \rightarrow 1$].

The impedance measurements can be utilized to understand the sensitivity of the sensing material system, as well as overall performance.[12] The same AC small-signal measurements can be used in detecting the magnitude of sensitivity via before and after values of the impedance. Thus, the sensitivity of the resistance and/or capacitance with respect to the concentration of the ambient gases can aid in determining the level of sensitivity of the material system. The impedance measurements overall provide direction to determining the capability of the sensing material, as well as the level of detection corresponding to the gas concentration.[12,13]

8. NANOSTRUCTURED METAL OXIDE CHEMICAL SENSORS

Nanoscience and nanotechnology pertain to the synthesis, characterization, exploration, interrogation, exploitation, and utilization of nanostructured materials, which are characterized by at least one dimension in the nanometer (1 nm = 10–9 m) range. Such nanostructured systems constitute a bridge between single molecules and infinite bulk systems. Individual nanostructures involve clusters, nanoparticles, nanocrystals, quantum dots, nanowires, and nanotubes, while collections of nanostructures involve arrays, assemblies, and super-lattices of individual nanostructures. The chemical and physical properties of nanomaterials can significantly differ from those of the atomic-molecular or the bulk materials of the same chemical composition.

The uniqueness of the structural characteristics, energetics, response, dynamics, and chemistry of nanostructures is novel and constitutes the experimental and conceptual background for the novel field of nanoscience. Suitable control of the properties and response of nanostructures can lead to new devices and technologies. The themes of nanoscience and nanotechnology are dual. First, there is the bottom-up approach of miniaturization of the components geared by the classic lecture of December 29, 1959 by Richard Feynman[79,80] at the Annual Meeting of the American Physical Society at the California Institute of Technology (Caltech). He stated that 'there is plenty of room at the bottom.' Second, the top-down approach of the self-assembly of molecular components geared where each molecular or nanostructured component exists.

All materials are composed of some building blocks, called grains. The key parameter that distinguishes nanostructured materials (powders or nanoparticles, metals, ceramics, and other solids) from conventional materials is the size of the constituent grains. The diameters of grains range between 1 to 100 nm for nanostructured materials, whereas those for conventional materials are from microns to millimeters. It is the size, complex interplay, and interaction at the interfaces of grains that enable these nanomaterials to exhibit unique or improved mechanical, optical, chemical, and electronic properties. Nonocrystalline materials can be classified into different categories depending on the number of dimensions that are nanosized (less than 100 nm). A possible classification is zero-dimension for clusters, mono-dimensional for nanowires; and two-dimensional for films.

There is a growing need to develop highly sensitive chemical sensors for applications, such as military reconnaissance and toxic waste removal. A promising route for improving device performance is to use nanostructured materials (e.g. nanoparticles, nanowires, nanotubes) as sensor building blocks. The use of nanostructures offers novel and advanced properties of oxide-based chemical sensors. If films of semiconducting metal oxides become ultrathin, contacts or catalytically active metal deposits reach nanosized dimensions, or if surfaces are functionalized with nanosized organic molecules, then the physical and chemical properties of nanostructures can be fundamentally different from the bulk material because of electron confinement and other quantum-effects. Similarly, finite-size effects and the enhanced density of structural imperfections can modify very significantly the sensing properties.

The discovery of such phenomena at the nanoscale and the development of new experimental and theoretical tools in the last few years of investigating these structures provided opportunities for scientific and technology developments in the nanostructured chemical sensors. In this section, main research lines of nanoscience and nanotechnology applied to semiconductor gas sensors will be reviewed, particularly SnO_2.

8.1 SnO_2 Nanowire Sensors

Kolmakov, et al.[81] reported the O_2 and CO- sensing properties based on an individual SnO_2 nanowire. Exposure to oxygen recreated the surface acceptor states, thereby reducing the nanowire's conductance, and restored the temperature dependence of the conductance to the exponential form typical of intrinsic semiconductors. Combustible gases like CO react with pre-adsorbed oxygen species to form carbon monoxide, reducing the steady-state surface oxygen concentration and donating a few electrons back into the bulk and resulting in an increased conductivity, which depends monotonically on the gas phase partial pressure of CO.

The electron exchange between the surface states and the bulk takes place within a surface layer, whose thickness is of the order of the Debye length, λ_D. In particular, experimental observations[81,82] indicated the rates of oxygen adsorption-desorption and catalytic oxidation of CO taking place on the surface of the SnO^2 nanowire, along with the specific reaction channel, were changed by varying the electron density inside the nanowire with the help of gate potential. It was found that manipulating the number of electrons inside a nanowire affected the chemical reactivity and selectivity of its surface.

By close analogy with the processes taking place in macroscopic metal oxide semiconductor field-effect transistor (MOSFET) gas sensors, Zhang, et al.[83] determined the electron transport properties of individual SnO_2 nanowires. These transport properties were configured over a wide range of temperature in various atmospheres comprising of the mixtures N_2-O_2-CO. Because of their large surface-to-volume ratios, the bulk electronic properties of the nanowires were found to be controlled almost entirely by the chemical processes taking place at their surface, which could in turn be modified by controlling the gate potential. Thus, the rate and extent of oxygen ionosorption and the resulting rate and extent of catalytic CO oxidation reaction on the nanowire's surface could be controlled and even entirely halted by applying a negative enough gate potential.

Wang, et al.[84] prepared a polycrystalline SnO_2 nanowires film for gas sensing. The nanowire film sensor exhibited high sensitivity and reversibility when exposed to ethanol vapor (~6 percent, Vethanol/Vair), 20 ppm CO, and 500 ppm H_2. The authors suggested that this could be attributed to the intrinsically small grain-size and high surface-to-volume ratios associated with the polycrystalline nanowires. A thin layer of the film close to the surface could be activated during gas detection due to the dense structure of a compact film. The small grains of SnO_2 in the nanowires allowed the sensors to be operated in the most sensitive, grain-controlled mode. Similarly, Barratto, et al.[85] tested the gas-sensing of SnO_2 nanowires. The response of the sensor was highly selective toward humidity and other polluting species, such as CO and NH_3. Wan, et al.[86] synthesized Sb-doped SnO_2 nanowires and exploited the application for gas sensors. It was found that the response range to ethanol was wide (10–1000 ppm) at 300 °C. The response and recovery

times to 10 ppm ethanol were only about 1 s and 5 s, respectively. Mulla and co-workers[87] reported the unique response towards NO_2 and LPG (liquefied petroleum gas) based on Ru-doped SnO_2 nanowires. The nanowires exhibited a highly selective sensing behavior towards NO_2 at room temperature. Mathur, et al.[88] studied the photo-sensing properties of SnO_2 nanowires and found that the photo-conductance of the SnO_2 nanowire showed a strong modulation that was dependent on the average radial dimensions.

8.2 SnO_2 Nanobelt Sensors

The first SnO_2 nanobelt-based gas sensor with a simple DC-resistance-measuring system was presented in 2002.[89] The transducer fabrication with a platinum interdigitated electrode structure was made using sputtering technique having shadow masking on alumina substrate. Then, a number of nanobelts was transferred onto the electrodes for electrical conductance measurements. The gases tested were CO, NO_2, and ethanol, which are important for environmental applications, breath analyzers, and food quality control. CO and ethanol increased conductivity, which is common for an n-type semiconductor, such as SnO_2, while opposite behavior was registered for NO_2.

Yu, et al.[90] recently published an article on SnO_2 nanobelts, proving their integration with micro-machined substrate, which is crucial if a real application is envisioned, and showing their sensitivity to nerve agent, an application of increasing interest for security reasons. Single nanobelt SnO_2 was transferred to a silicon micro-system device fabricated with a top-down approach. The resistance of the nanobelt increased by 5 percent when added to 78 ppb of dimethyl methylphosphonate (DMMP), a nerve agent stimulant.

8.3 SnO_2 Nanotube Sensors

Recently Liu and Liu[91] reported a single, square-shaped SnO^2 nanotube gas sensor for ethanol, bridging two interdigitated Pt electrodes. Huang, et al.[92] studied responses of a SnO^2 nanotube sheet sensor to 100 ppm H_2, 100 ppm CO, and 20-ppm ethylene oxide. The sheet (0.2 mm thick) was about 2 mm×4 mm in size and was fixed with gold paste onto an alumina substrate attached with gold electrodes having a gap of 1 mm.

9. CONCLUSIONS

The number one failure mechanism for propulsion systems is leakage. Confined space and cabin air quality are of chief concern for a crew in orbit. Chemical sensors are used widely in many fields of endeavor. In the present review various kinds of chemical sensors are reviewed. The principles of a metal-oxide sensor are explained in detail. Ways to improve sensor performance are also given. This review includes an exploratory study carried out at AAMU on polycrystalline binary composite films: SnO_2-WO_3, SnO_2-In_2O_3, and SnO_2-ZnO for the detection of isopropanol. Samples are prepared for thick film transfer (screen-printing) onto alumina substrates. Binary thick film samples of SnO_2 with WO_3 show the superior sensor properties of increased sensitivity and reduced response time. Furthermore, operating temperature for thick film polycrystalline sensors is lowered from ~500 °C to 140 °C. Current research status of chemical sensors based upon new types of nanostructured materials, such as nanowires, nanobelts, and nanotubes based on SnO_2, is also reported.

REFERENCES

1. Gong, H., Wang, Y.J., Teo, S.C., and Huang, L.: "Interaction of Thin-Film Tin Oxide Gas Sensor and Five Organic Vapors," S*ensors and Actuators B: Chemical*, Vol. 54, pp. 232–235, 1999.

2. Ho, C.K., Itamura, M.T., Kelley, M., and Hughes, R.C.: "Report: Review of Chemical Sensors for In-situ Monitoring of Volatile Contaminants," *Sandia Report* SAND2001-0643, 2001.

3. Z. Tianshu, P. Hing, Y. Li, and Z. Jiancheng: "Selective Detection of Ethanol Vapor and Hydrogen using Cd-Doped SnO_2-Based Sensors," *Sensors and Actuators B: Chemical*, Vol. 60, pp. 208–215, 1999.

4. Coles, G.S.V., Williams, G., and Smith, B.: "Selectivity Studies on Tin Oxide Based Semiconductor Gas Sensors," *Sensors and Actuators B: Chemical*, Vol. 3, pp. 7–14, 1991.

5. Oyabu, T., Ohta, Y., and Kurobe, T.: "Tin Oxide Gas Sensor and Counter Measure System against Accidental Gas Leaks," *Sensors and Actuators B: Chemical*, Vol. 9, pp. 301–312, 1986.

6. Yamamoto, N., Tonomura, S., Matsuoka, T., and Tsubomura, H.: "The Effect of Reducing Gases on the Conductivities of Metal Oxides Semiconductors," *Japanese Journal of Applied Physics*, Vol. 20, pp. 721–726, 1981.

7. Yang, Y.K. and Lee, J.J.: "A Tin Oxide Thin Film Sensor with High Ethanol Sensitivity," *Thin Solid Films*, Vol. 169, pp. 51–56, 1989.

8. Ihokura, K. and Watson, J.: "Stannic Oxide Gas Sensor," CRC Press, Ann Arbor, MI, 1994.

9. Yu, J.H. and Choi, G.M.: "Electrical and CO Gas Sensing Properties of ZnO-SnO_2 Composites," *Sensors and Actuators B: Chemical*, 52 (3), pp. 251–256, 1998.

10. de Lacy Costello, B.P.J., Ewen, R.J., Jones, P.R.H., et. al.: "A Study of the Catalytic and Vapor-Sensing Properties of Zinc Oxide and Tin Oxide in Relation to 1-Butanol and Dimethyldisulphide," *Sensors and Actuators B: Chemical*, 61 (1–3), pp. 199–207, 1999.

11. Yu, J.H. and Choi, G.M.: "Electrical and CO Gas Sensing Properties of ZnO/SnO_2 Hetero-Contact," *Sensors and Actuators B: Chemical*, Vol. 61, pp. 1–3, 1999.

12. Currie, J.R.: "Studies of Metal Oxide Chemical Sensors for the Detection of Volatile Organic Compounds," Ph.D. Dissertation, Alabama A&M University, Huntsville, AL, 2008.

13. Currie, J.R., Batra A.K., Alim, M.A., Aggarwal, M.D., and Lal, R.B.: "Impedance Studies of Polycrystalline Tin Oxide," *Journal of Materials Science: Materials in Electronics*, Vol. 18, pp. 433–439, 2007. Currie, J.R., Batra, A.K., Alim, M.A., Aggarwal, M.D., and Lal, R.B.: "Erratum: Impedance Studies of Polycrystalline Tin Oxide," *Journal of Materials Science: Materials in Electronics*, Vol. 18, p. 899, 2007.

14. Hagleitner, C., Hierlemann, A., Lange, D., Kummer, A., Kerness, N., Brand, O., and Baltes, H.: "Smart Single Chip Gas Sensor Microsystem," *Nature*, Vol. 414, pp. 293–296, 2001.

15. Krishna, G.M.: "Development of Tactile Sensors Based on Piezoelectric Resonance and Surface Acoustic Wave Techniques," M.Sc. (Engineering) Thesis, Indian Institute of Science, Bangalore, India (2001). Krishna, G.M. and Rajanna, K.: "Tactile Sensors Based on Piezoelectric Resonance," *IEEE Sensor Journal*, 4 #5, pp. 691–697, 2004.

16. Vellekoop, M., Lubking, G., and Venema, A.; "Acoustic Wave Based Monolithic Microsensors," *Proceeding of the IEEE Ultrasonics Symposium*, Vol. 1, pp. 565–574, 1994.

17. Martin, S., Frye G., Spates, J., and Butler, M.; "Gas Sensing with Acoustic Devices," *Proceeding of the IEEE Ultrasonics Symposium*, Vol. 1, pp. 423–434, 1996.

18. White, R., Wicher, P., Wenzel, W., and Zellers, E.: "Plate Mode Ultrasonic Oscillator Sensors," *IEEE Transactions on Ultrasonics, Ferroelectrics and Frequency Control*, 34 (2), pp. 162–171.

19. Wenzel, S., Martin, B., and White, R.: "Generalized Lamb-Wave Multisensor," *Proceeding of the IEEE Ultrasonics Symposium*, Vol. 1, pp. 563–567, 1988.

20. Grate, J., Wenzel, S., and White, R.: "Flexural Plate Wave Devices for Chemical Analysis," *Analytical Chemistry*, Vol. 63, pp. 1,552–1,561, 1991.

21. Wenzel, S. and White, R.: "Flexural Plate Wave Sensor: Chemical Vapor Sensing and Electostrictive Excitation," *Proceeding of the IEEE Ultrasonics Symposium*, Vol. 1, pp. 595–598, 1989.

22. Andle, J., Vetelino, J., Lec, R., and McAllister, D.: "An Acoustic Plate Mode Iimmunosensor," *Proceeding of the IEEE Ultrasonics Symposium*, Vol. 1, 579–584, 1989.

23. Costello, B., Martin, B., and White, R.: "Ultrasonic Plate Waves for Biochemical Measurements," *Proceeding of the IEEE Ultrasonics Symposium*, Vol. 1, pp. 977–981, 1989.

24. Andle, J. and Vetelino, J.: "Acoustic Wave Biosensors," *Sensors and Actuators A: Physical*, Vol. 44, pp. 167–176, 1994.

25. Grate, J., Martin, S., and White, R.: "Acoustic Wave Microsensors: Part 1," *Analytical Chemistry,* 65 (21), pp. 940A–948A, 1993.

26. Grate, J., Martin, S., and White, R.: "Acoustic Wave Microsensors: Part 2," *Analytical Chemistry*, 65 (22), pp. 987A–996A, 1993.

27. Slobodonik, A.: "SAW and SAW Materials," *Proceedings of the IEEE*, 64 (5), pp. 581–595, 1976.

28. Shimizu, Y.: "Current Status of Piezoelectric Substrate and Propagation Characteristics for SAW Devices," *Japanese Journal of Applied Physics: Part B*, 32 (5), pp. 2,183–2,187, 1993.

29. Tirole, N., Choujaa, A., Hauden, D., Martin, G., Blind, P., Froelicher, M., Pommier, J., and Cachard, A.: "Lamb Waves Pressure Sensor using AlN/Si Structure," *Proceeding of the IEEE Ultrasonics Symposium,* Vol. 1, pp. 371–374, 1993.

30. Solie, L.: "Tapered Transducers - Design and Applications," *Proceeding of the IEEE Ultrasonics Symposium*, Vol. 1, pp. 27–37, 1998.

31. Lee, Y., Lee, S., and Roh, Y.: "Design of Withdrawal-Weighted SAW Filters," *IEEE Transactions on Ultrasonics, Ferroelectrics and Frequency Control*, 49 (3), pp. 337–344, 2002.

32. Wenzel, S., and White, R.: "Analytical Comparison of the Sensitivities of Bulkwave, Surface-Wave and Flexural Plate-Wave Ultrasonic Gravimetric Sensors," *Applied Physics Letters*, 54 (20), pp. 1,976–1,978, 1989.

33. Black, J., Chen, B., Quinn, R., White, R., and Madou, M.: "Comparison of the Performance of FPW and SAW Devices as the Detector in a Gas Chromatograph," *Proceeding of the IEEE Ultrasonics Symposium*, Vol. 1, pp. 435–440, 2000.

34. Anisimkin, V., Veradi, P., and Verona, E., "New Properties of the SAW Gas Sensing", *Proceeding of the IEEE Ultrasonics Symposium*, Vol. 1, pp. 405–408, 1997.

35. van der Meer, P., Meijer, G., Vellekoop, M., Kerkvliet, H., and van den Boom, T.: "A Temperature-Controlled Smart Surface-Acoustic-Wave Gas Sensor," *Sensors and Actuators A: Physical*, 71 (1–2), pp. 27–34, 1998.

36. Rapp, M., Reibel, J., Stier, S., Voigt, A., and Bahlo, J.: "SAGAS: Gas Analyzing Sensor Systems Based on Surface Acoustic Wave Devices - An Issue of Commercialization of SAW Sensor Technology," *Proceedings of the IEEE International Frequency Control Symposium: IEEE International*, pp. 129–132, 1997.

37. Caliendo, C., D'Amico, A., Varadi, P., and Verona, E.: "Surface Acoustic Wave H_2 Sensor on Si Substrate," *Proceeding of the IEEE Ultrasonics Symposium*, Vol. 1, pp. 569–574, 1988.

38. Jakubik, W., Urbanczyk, M., Kochowski, S., and Bodzenta, J.: "Bilayer Structure for Hydrogen Detection in a SAW Sensor System," *Sensors and Actuators B: Chemical*, Vol. 82, pp. 265–271, 2002.

39. Zellers, E., White, R., and Wenzel, S.: "Computer Modeling of Polymer Coated ZnO/Si SAW and Lamb Wave Chemical Sensors," *Sensors and Actuators A: Materials*, Vol. 14, pp. 35–45, 1988.

40. <http://www.sandia.gov/mstc/technologies/microsensors/techinfo.html>.

41. Kohl, D.: "Topical Review: Function and Applications of Gas Sensors," *Journal of Applied Physics*, 34, R125–R149, 2001.

42. Tabib-Azar, M., Sutapun, B., Petrick, R., and Kazemi, A.: "Highly Sensitive Hydrogen Sensors using Palladium Coated Fiber Optics with Exposed Cores and Evanescent Field Interactions," *Sensors and Actuators B: Chemical*, Vol. 56, pp. 158–163, 1999.

43. Mari, C., Barbi, G., and Sberveglieri, G., "Gas Sensors-Principles: Operation and Developments," Kluwer Academic Publishers, Dordrecht, p. 329, 1992.

44. Ivers-Tiffée, E., Härdtl, K.H., Menesklou, W., and Riegel, J.: "Principles of Solid State Oxygen Sensors for Lean Combustion Gas Control," *Electrochimica Acta*, 47 (5), pp. 807–814, 2001.

45. *Semiconductor Sensors*, Sze, S.M., ed., John Wiley and Sons, Inc., New York (1994).

46. Mark, P., and Windischmann, H.: "A Model for the Operation of a Thin-Film SnOx Conductance-Modulation Carbon Monoxide Sensor," *Journal of the Electrochemical Society*, 126 #4, pp. 627–633, 1979.

47. Dieguez, A., Romano-Rodrguez, A., Mornante, J.R., Kappler, J., Barsan, N., and Gopel, W.: "Nanoparticle Engineering for Gas Sensor Optimization: Improved Sol-Gel Fabricated Nanocrystalline SnO_2 Thick Film Gas Sensor for NO_2 Detection by Calcinations, Catalytic Metal Introduction and Grinding Treatments," *Sensors and Actuators B: Chemical*, Vol. 60, pp. 125–137, 1999.

48. Xu, C., Tamaki, J., Miura, N., and Yamazoe, N.: "Grain-size Effects on Gas Sensitivity of Porous SnO_2-Based Elements," *Sensors and Actuators B: Chemical*, 3 #2, pp. 147–155, 1991.

49. S. Nocoletti; "Tin-Oxide Thin Film Sensors for Aromatic Hydrocarbon Detection," *Journal of the American Ceramic Society*, 83 (5), pp. 1,201–1,206, 1999.

50. Williams, D.E. and Mosely, P.T.: "Dopant Effects on the Response of Gas-Sensitive Resistors utilizing Semiconducting Oxides," *Journal of Materials Chemistry*, Vol. 1, pp. 809–814, 1991.

51. Wollenstein, J.: "Materials Properties and the Influence of Metallic Catalysts at the Surface of Highly Dense SnO_2 Film," *Sensors and Actuators B: Chemical*, Vol. 70, pp. 196–202, 2000.

52. Vlachos, D.S., Papadopoulos, C.A., and Avaritsiotis, J.N.: "On the Electronic Interaction between Additives and Semiconducting Oxide Gas Sensors," *Applied Physics Letters*, 69 (5), pp. 650–652, 1996.

53. Zhang, J. and Colbow, K.: "Surface Silver Clusters as Oxidation Catalysts on Semiconductor Gas Sensors," *Sensors and Actuators B: Chemical*, Vol. 4, pp. 47–52, 1997.

54. Montmeat, P.: “The Influence of Platinum Membrane on the Sensing Properties of a Tin Dioxide Thin Film,” *Sensors and Actuators B: Chemical*, 84 #2-3, pp. 148–159, 2002.

55. Papadopoulos, C.A. and Avaritsiotis, J.N.: “A Model for Gas Sensing Properties of Tin Oxide Thin Films with Surface Catalysts,” *Sensors and Actuators B: Chemical*, Vol. 48, pp. 201–210, 1995.

56. Weimar, U. and Goepel, W.: “AC Measurements on the Tin Oxide Sensors to Improve Selectivities and Sensitivities,” *Sensors and Actuators B: Chemical*, Vol. 26, pp. 13–18, 1995.

57. Morrison, S.R.: “Selectivity in Semiconductor Gas Sensors,” *Sensors and Actuators B: Chemical*, Vol. 12, pp. 425–440, 1987.

58. <http://ceiba.cc.ntu.edu.tw/catalysis/course/Chap6.pdf>.

59. Srivastava, R.K.: “Sensing Mechanism in Tin Oxide Based Thick-Film Gas Sensors,” *Sensors and Actuators B: Chemical*, Vol. 21, pp. 213–218, 1994.

60. Waltson, J., Ihokura, K., and Cole, S.V.: “Tin Oxide Gas Sensor,” *Measurement Science and Technology*, Vol. 4, pp. 711–719, 1993.

61. Babaei, F.H. and Orvatinia, M.: “Analysis of Thickness Dependence of the Sensitivity in Thin Film Resistive Gas Sensors,” *Sensors and Actuators B: Chemical*, Vol. 89, pp. 256–261, 2003.

62. Becker, T., Ahlers, S., Braunmühl, C.B.-V. , Müller, G., and Kiesewetter, O.: “Gas Sensing Properties of Thin- and Thick-Film Tin Oxide Materials,” *Sensors and Actuators B: Chemical*, Vol. 77, pp. 55–61, 2001.

63. Llobet, E.: “Multicomponent Gas Mixture Analysis using a Single Tin Oxide Sensor and Dynamic Pattern Recognition,” *IEEE Sensor Journal*, 1(3), pp. 207–213, 2001.

64. Lim, J.W.: “Heating Power Controlled Micro Gas Sensor Array,” *Sensors and Actuators B: Chemical*, Vol. 77, pp. 139–144, 2000.

65. Hagletiner, C.: “Smart Single-Chip Sensor Microsystem,” *Nature*, Vol. 414, pp. 293–296, 2001.

66. Ogawa, H., Abe, A., Nishikawa, M., and Hayakawa, S.; “Electrical Properties of Tin Oxide Ultrafine Particle Films,” *Journal of the Electrochemical Society*, 128 #9, pp. 2,020–2,025, 1981.

67. Cole, K.S., and Cole, R.H.: “Dispersion and Absorption in Dielectrics: Alternating Current,” *Journal of Chemical Physics*, Vol. 9, pp. 341–351, 1941.

68. Alim, M.A.: “Electrical Characterization of Engineering Materials,” *Active and Passive Electronic Components*, 19 #3, pp. 139–169, 1996.

69. Smyth, C.P.: *Dielectric Behavior and Structure*, McGraw-Hill Book Company, New York, 1955.

70. von Hippel, A.R.: *Dielectrics and Waves*, John Wiley & Sons, Inc., New York, 1954.

71. Goepel, W. and Schierbaum, K.D.: "SnO_2 Sensors: Current Status and Future Prospects," *Sensors and Actuators B: Chemical*, Vol. 26, pp. 1–12, 1995.

72. Shishiyanu, S.T., Shishiyanu, T.S., and Lupan, O.I.: "Sensing Characteristics of Tin-Doped ZnO Thin Film as NO_2 Gas Sensor," *Sensors and Actuators B: Chemical*, Vol. 107, pp. 379–386, 2004.

73. Azad, A.M., Akbar, S.A., Mhaisalkar, S.G., Birkefeld, L.D., and Goto, K.S.: "Solid-State Gas Sensors: A Review," *Journal of the Electrochemical Society*, Vol. 139, pp. 3,690–3,704, 1992.

74. Xu, J., Pan, Q., Shun, Y.A., Tan, Z., "Grain-size Control and Gas Sensing Properties of ZnO Gas Sensor," *Sensors and Actuators B: Chemical*, Vol. 66, pp. 277–279, 2000.

75. Arshak, K. and Gaidan, I.; "Development of a Novel Gas Sensor Based on Oxide Thick Films," *Materials Science and Engineering B*, Vol. 118, pp. 44–49, 2005.

76. "Gas Sensors: Principles, Operation and Developments," Giorgio Sberveglieri edited, Springer, 1992.

77. Kugishima, M., Shimanoe, K., and Yamazoe, N.: "C_2H_4O Sensing Properties for Thick Film Sensor using La_2O_3-Modified SnO_2," *Sensors and Actuators B: Chemical*, Vol. 118, pp. 171–176, 2006.

78. Park, S.S. and Mackenzie, J.D.: "Thickness and Microstructure Effects on Alcohol Sensing of Tin Oxide Thin Films," *Thin Solid Films*, Vol. 274, pp. 154–159, 1996.

79. Jortner, J., and Rao, C.N.R.: "Nanostructured Advanced Materials – Perspectives and Directions," *Pure and Applied Chemistry*, 74 #9, pp. 1,491–1,506, 2002.

80. <http://www.zyvex.com/nanotech/feynman.html>.

81. Kolmakov, A., Zhang, Y., Cheng, G., and Moskovits, M.: "Detection of CO and O_2 using Tin Oxide Nanowires Sensors," *Advanced Materials*, 15 #12, pp. 997–1,000, 2003.

82. Zhang, Y., Kolmakov A., Chretien, S., Metiu, H., and Moskovits, M.: "Control of Catalytic Reactions at the Surface of a Metal Oxide Nanowire by Manipulating Electron Density Inside It," *Nano Letters*, Vol. 4, pp. 403–407, 2004.

83. Zhang, Y., Kolmakov, A., Lilach, Y. , and Moskovits, M.: "Electronic Control of Chemistry and Catalysis at the Surface of an Individual Tin Oxide Nanowire," *Journal of Chemical Physics B*, Vol. 109, pp. 1,923-1,929, 2005.

84. Wang, Y.L., Jiang, X.C., and Xia, Y.N.: "A Solution-Phase, Precursor Route to Polycrystalline SnO_2 Nanowires that can be used for Gas Sensing under Ambient Conditions," *Journal of the American Chemical Society*, Vol. 125, pp. 16,176–16,177, 2003.

85. Barratto, C., Comini, E., Faglia, G., et al.: "Metal Oxide Nanocrystals for Gas Sensing," *Sensors and Actuators B: Chemical*, Vol. 109, pp. 2–6, 2005.

86. Wan, Q., and Wang, T.H., "Single-Crystalline Sb-Doped SnO_2 Nanowires: Synthesis and Gas Sensor Application," *Chemical Communications*, pp. 3,841–3,843, 2005.

87. Ramgir, N.S., Mulla, I.S., and Vijyamohanan, K.P.: "A Room Temperature Nitric Oxide Sensor Actualized from Ru-Doped SnO_2 Nanowires," *Sensors and Actuators B: Chemical*, Vol. 107, pp. 708–715, 2005.

88. Mathur, S., Barth, S., Shen, H., Pyun, J.C., and Werner, U.: "Size-Dependant Photo-Conductance in SnO_2 Nanowire," *Small*, Vol. 1, pp. 713–717, 2005.

89. Comini, E., Faglia, G., Sberveglieri, G., Pan, Z., and Wang, Z.L.: "Stable and Highly Sensitive Gas Sensors Based on Semiconducting Oxide Nanobelts," *Applied Physics Letters*, Vol. 81, p. 1869, 2002.

90. Yu, C., Hao, Q., Saha, S., Shi, L., Kong, X., and Wang, Z.L., "Integration of Metal Oxide Nanobelts with Microsystems for Nerve Agent Detection," *Applied Physics Letters*, 86, 063101, 2005.

91. Liu, Y., and Liu, M.L.: "Growth of Aligned Square-Shaped SnO_2 Tube Arrays," *Advanced Functional Material*, Vol. 15, pp. 57–62, 2005.

92. Huang, J., Matsunaga, N., Shimanoe, K., Yamazoe, N., and Kunitake, T.: "Nanotubular SnO_2 Templated by Cellulose Fibers: Synthesis and Gas Sensing," *Chemistry of Materials*, Vol. 17, pp. 3,513–3,518, 2005.

REPORT DOCUMENTATION PAGE

Form Approved
OMB No. 0704-0188

1. REPORT DATE *(DD-MM-YYYY)*	2. REPORT TYPE	3. DATES COVERED *(From - To)*
01-10-2008	Technical Memorandum	

4. TITLE AND SUBTITLE

Micro- and Nanostructured Metal Oxide Chemical Sensors for Volatile Organic Compounds

5a. CONTRACT NUMBER

5b. GRANT NUMBER

5c. PROGRAM ELEMENT NUMBER

6. AUTHOR(S)

M.A. Alim, B.G. Penn, J.R. Currie, Jr., A.K. Batra,* and M.D. Aggarwal*

5d. PROJECT NUMBER

5e. TASK NUMBER

5f. WORK UNIT NUMBER

7. PERFORMING ORGANIZATION NAME(S) AND ADDRESS(ES)

George C. Marshall Space Flight Center
Marshall Space Flight Center, AL 35812

8. PERFORMING ORGANIZATION REPORT NUMBER

M–1244

9. SPONSORING/MONITORING AGENCY NAME(S) AND ADDRESS(ES)

National Aeronautics and Space Administration
Washington, DC 20546–0001

10. SPONSORING/MONITOR'S ACRONYM(S)

NASA

11. SPONSORING/MONITORING REPORT NUMBER

NASA/TM—2008–215579

12. DISTRIBUTION/AVAILABILITY STATEMENT

Unclassified-Unlimited
Subject Category 23
Availability: NASA CASI 443–757–5802

13. SUPPLEMENTARY NOTES

Prepared by EV43, Integrated System Health Management and Sensors Branch
*Alabama A&M University, Normal, Alabama 35762

14. ABSTRACT

Aeronautic and space applications warrant the development of chemical sensors which operate in a variety of environments. This technical memorandum incorporates various kinds of chemical sensors and ways to improve their performance. The results of exploratory investigation of the binary composite polycrystalline thick-films such as SnO_2-WO_3, SnO_2-In_2O_3, SnO_2-ZnO for the detection of volatile organic compound (isopropanol) are reported. A short review of the present status of the new types of nanostructured sensors such as nanobelts, nanorods, nanotube, etc. based on metal oxides is presented.

15. SUBJECT TERMS

chemical sensors, micro- and nanostructured sensors, sensors for volatile organic compounds

16. SECURITY CLASSIFICATION OF:			17. LIMITATION OF ABSTRACT	18. NUMBER OF PAGES	19a. NAME OF RESPONSIBLE PERSON
a. REPORT	b. ABSTRACT	c. THIS PAGE			STI Help Desk at email: help@sti.nasa.gov
U	U	U	UU	62	19b. TELEPHONE NUMBER *(Include area code)* STI Help Desk at: 443-757-5802

National Aeronautics and
Space Administration
IS20
George C. Marshall Space Flight Center
Marshall Space Flight Center, Alabama
35812